RAPID CONCRETE PAVEMENT SPALL REPAIR

USING 3D SCANNING AND 3D PRINTING TECHNOLOGIES

A Dissertation

by

JAEHEUM YEON

Submitted to the Office of Graduate and Professional Studies of
Texas A&M University
in partial fulfillment of the requirements for the degree of

DOCTOR OF PHILOSOPHY

Chair of Committee,	Julian Kang
Co-Chair of Committee,	Wei Yan
Committee Members,	John Walewski
	Takashi Yamauchi
Head of Department,	Robert Warden

May 2017

Major Subject: Architecture

ABSTRACT

Conventional methods for repairing damages to concrete pavement require a certain amount of time, regardless of the scale of the harm. The area must first be cleaned; this means that the damaged section must be separated from the surrounding area by sawing around its edges. The failing concrete is then broken up and removed. After pouring fresh concrete into the resulting hole, the U.S. Department of Transportation recommends waiting at least seven days before proceeding to the next step. Vehicles must be detoured for the entirety of this period, which often results in vehicle depreciation by as much as $140,000 per a repair project. Considering the indirect losses that can be caused by this process, stakeholders often find it difficult to decide when palm-size spall damage should be repaired. Many government agencies wait until the damaged sections become severe enough to justify a road closure.

This dissertation presents a novel idea for speeding up the repair process for palm-size spall damage of concrete pavement: the use of 3D scanning and 3D printing. This study presents the suggested method to repair small damage on a concrete pavement using a prefabricated concrete segment tailored for the damaged area. The suggested method begins with scanning the damaged area using photogrammetry to get a 3D model. After that, printing out the obtained 3D model using a 3D printer. The output of a 3D printer is used as a formwork. And then pouring concrete in the formwork and curing a concrete segment tailored for the damaged area. Last, plug a pre-fabricated concrete segment in the damaged area after the adhesive is applied.

However, each step of this spall repair sequence has its tolerance such as the level of the accuracy of the 3D scanner and the shrinkage of the output of the 3D printer. When these errors are accumulated, we can simply assume that there will be a certain space between the bottom of the prefabricated concrete segment and the surface of the spall when the concrete segment is later inserted into the spall. This space will be filled with an adhesive. But it is not known yet to what extent the adhesive layer will be formed. However, it can be predicted that the thickness of the adhesive layer will have some effect on how it will hold the concrete segment. Therefore, this study identifies the maximum shear stress and proposes a modified slant shear test method to experimentally investigate the influence of bond line thickness of epoxy-resin adhesive on shear strength when the glue applied to a concrete adherend. Also, this research investigates the attached concrete segment is strong enough to handle the maximum applied stress.

The conclusions of this research are that first, it was found that having an adhesive layer between a concrete segment and a spall has better adhesive strength than a perfect fit between a concrete segment and a spall. Also, it was found that the spall repair method using 3D printer is sufficiently realistic. Last, the ultimate shear strength of three epoxy-resin adhesives that were used in this study can be predicted when the measured bond line thickness applied to the variable of the determined mathematical relationships of each adhesive.

ACKNOWLEDGEMENTS

I could not have completed this journey without the help of my committee members. First, I sincerely thank Dr. Julian Kang for giving me this opportunity and helping me in countless ways during this process. Thank you also to Dr. Wei Yan, who has always given me invaluable, heartfelt advice. I am so grateful to Dr. John Walewski for his assistance during both my master's and doctoral studies. Finally, I am deeply grateful to Dr. Takashi Yamauchi, without whose help I could not have finished my degree.

I would also like to thank my parents for helping me throughout my life. I hope this accomplishment will serve as a small reward for all your suffering. I am also thankful for my brother, who walked this road before me and whose wonderful life is an example of the reward that comes from hard work.

Lastly, I would like to thank my wife, Jayoung Kim, who always believed in me and who came to the other side of the globe so that I could achieve this goal. Finally, I am grateful for my son, Daniel J. Yeon, who is my tiny enlightenment and the driving force of my life.

CONTRIBUTORS AND FUNDING SOURCES

Contributors

This work was supervised by a dissertation committee consisting of Dr. Julian Kang (Chair) of the Department of Construction Science and Dr. Wei Yan (Co-Chair) of the Department of Architecture.

All work for the dissertation was completed by the student, under the advisement of Dr. Julian Kang of the Department of Construction Science and Dr. Wei Yan of the Department of Architecture.

Funding Sources

There are no outside funding contributions to acknowledge related to the research and compilation of this document.

NOMENCLATURE

3D	Three-dimensional
ASTM	American Society for Testing and Materials
BS EN	British Standard European Norm
ISO	International Organization for Standardization
LVDT	Linear Variable Differential Transformer
PPI	Producer Price Index
US DOT	United States Department of Transportation
UTM	Universal Testing Machine

TABLE OF CONTENTS

Page

LIST OF FIGURES

Page

LIST OF TABLES

Page

1. INTRODUCTION

1.1 Spall Damage to Concrete Pavement

Concrete pavement is usually divided into slabs with transverse joints, in order to accommodate its expansion and contraction (Houben 2009). The edges of these slabs can often become damaged at the intersections, mainly due to heavy vehicles traveling at high rates of speed. Palm-sized concrete chips or chunks broken off the surface (see Figure 1) result in depressions called "spalls;" if not properly and timely treated, these spalls can cause serious structural harm to the slabs (McVay 1988) (Basham et al. 2001).

Figure 1 Beginning of a Spall (Fowler et al. 2008)

Currently, partial depth damage repair is the most commonly adopted method used to rehabilitate spall damages found on the surface of concrete pavement (Basham et al. 2001). As shown in Figure 2, once the damaged area is separated from the remainder of the slab via a milling machine, the damaged section is broken up with a chipping

device and the concrete debris are blown away by an air compressor. Concrete is then poured into the cleaned section. To prevent water infiltration, the edges of the repaired area are filled in with a waterproof agent. A white-pigmented curing compound is then applied to the repaired area, in order to prevent drying shrinkage and water (Basham et al. 2001).

Figure 2 Mill-and-Patch Repair Sequence (FHA 1994)

1.2 Challenge

Areas rehabilitated via the saw-and-patch method tend to be more stable and last longer than when spall damage is filled in with asphalt. However, this process demands

significant time and expensive equipment. In addition to the energy required to fix the spall damage itself, the slab must be isolated until the fresh concrete applied to the area is fully cured. The time required for the concrete hydration process varies depending on the type of cement used, but traffic must be detoured for at least seven days, until the white curing compound is applied to the patch (Basham et al. 2001).

While the pavement is being repaired, the adjacent road must also be closed so that the workspace can be secured; this often results in traffic jams, which have a negative impact on the economy. According to a report from the US DOT (US DoT 2015), this type of traffic impediment can result in up to a $20,000 loss per day (see Table 1). If the road is blocked for seven days (as is recommended), the loss can easily reach $140,000.

Table 1 Daily Time-Related Vehicle Depreciation

Vehicel Type	Time-Related Depreciation ($/hr) in 1995 $	PPI 1995	PPI 2015	Adjustment Factor =PPI 2015/PPI 1995	Total Depreciation ($/hr) in 2015 $	Simple Average of Hourly Costs in 2015 $ ($/hr)	Estimated Delay Time for All Vehicles (vehicle-hours/day)	Percentages for Vehicle Types (%)	Estimated Delay Time for Vehicle Types (vehicle-hours/day)	Estimated Time-Related Depreciation Costs ($/day)
Small Autos	1.09	134.1	135.4	1.0097	1.1006	1.33912	10192.6	0.88	8969.488	12011.219
Medium-Sized to Large Autos	1.45	159	173	1.0881	1.5777					
Four-Tire Single Unit Trucks	1.9	144.1	219.8	1.5253	2.8981	3.47012		0.08	815.408	2829.5676
Six-Tire Trucks	2.65	144.1	219.8	1.5253	4.0421					
3+Axles Combination Trucks	7.16	124.5	202	1.6225	11.617	10.6706		0.04	407.704	4350.4364
3 or 4 Axles	6.41	124.5	202	1.6225	10.4					
5 + Axles	6.16	124.5	202	1.6225	9.9945					
Estimated Time-Related Depreciation Costs for All Vehicles per Day										19191.223
										20000

1.3 Motivation

Dentists now use 3D scanning and printing technologies to fill cavities in teeth. As shown in Figure 3, they employ a laser to scan the 3D geometry of the cavity and a 3D printer to produce the filling, which together greatly facilitates the cavity treatment process (Miyazaki et al. 2009).

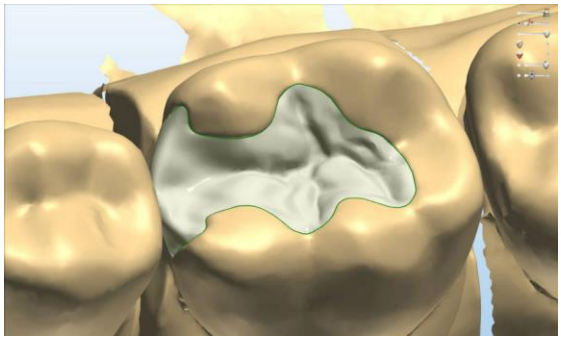

Figure 3 Using CAD/CAM Technology to Fill a Cavity (Carr 2009)

The purpose of this research is to determine if a similar process could be employed to apply this type of technology to spall damage repair. The steps discussed below were followed to test this theory.

1.3.1 Roadway Block

For the safety of the job site crew members, the roadway was blocked by barricades around the spall (see Figure 4).

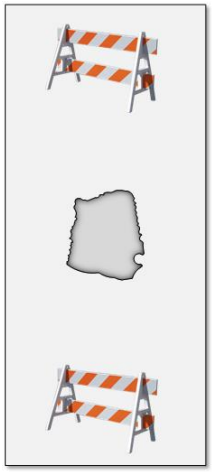

Figure 4 Traffic Blockage

1.3.2 3D Scanning Technology Used to Create a 3D Spall Model

The spall then was scanned using photogrammetry in order to generate a three-dimensional spall model. An 8-megapixel iPhone 6 camera was employed to take photos of the spall damage. The details of the photogrammetry scanning sequence are discussed below.

1.3.3 Camera Positioning

This type of photogrammetry requires that the photos be taken in bright daylight, in order to generate a high-resolution 3D model. A camera was used to take a series of photos around the spall, each at a 30^{o} angle (as shown in Figure 5). Because a spall is like a dent in the concrete, its photogrammetry requires more camera positions than what would be required of a convex surface (Dai and Lu, 2008).

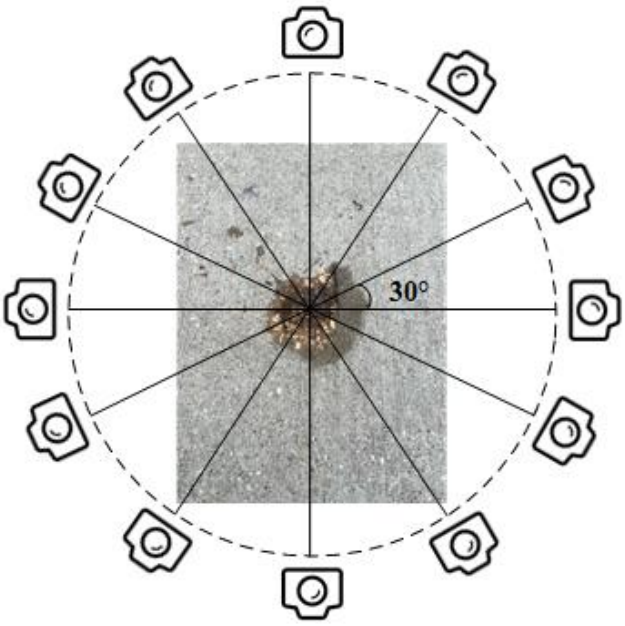

Figure 5 Horizontally-Rotated Camera Positions

Since a spall has depth, after the photos were taken from the horizontal camera positions, the camera's orientation was then moved vertically; this ensured that the photos adequately represented the depth of the damage (see Figure 6) (Dai and Lu, 2008).

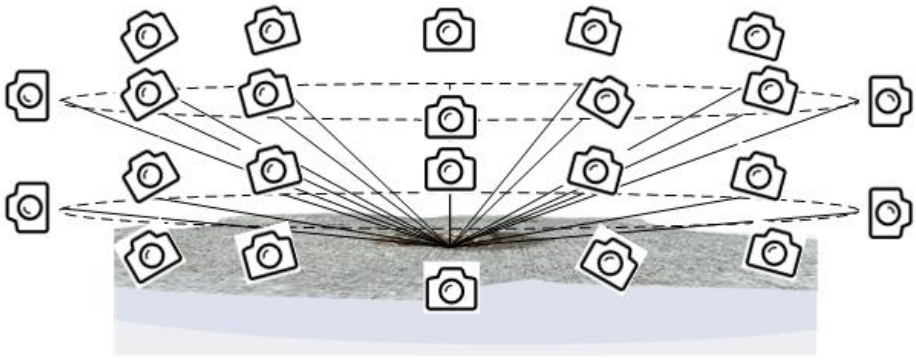

Figure 6 Vertically-Rotated Camera Positions

1.3.4 Photogrammetry Via Commercial Software

The photos were then uploaded into Autodesk ReMake a commercial 3D modeling software package, which stitched the photos together to map the 3D spall model (see Figure 7).

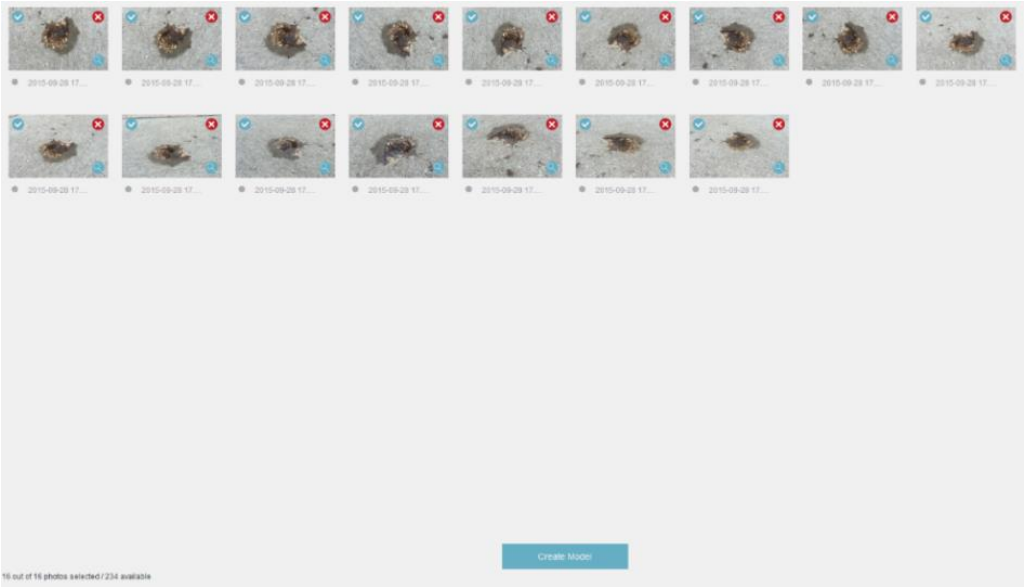

Figure 7 Commercial Software Used to Stitch Together the Photos

1.3.5 3D Model

The amount of time required for the stitching process depends upon the size of the spall, number of photos taken, and resolution of the camera. In this example, the scale of the 3D model was controlled as much as possible, because Autodesk ReMake does not create 3D models in actual size when they are initially generated. Thus, the

maximum diameter of the actual spall was measured as the standard, which was then used to control the scale of the 3D model. Since the exact locations of the two points selected to measure the maximum diameter of the spall could not be recognized when the 3D model was created, two objects were placed as indicators of where the maximum width was measured; those objects were included at the time the photos were taken, as shown in Figure 8.

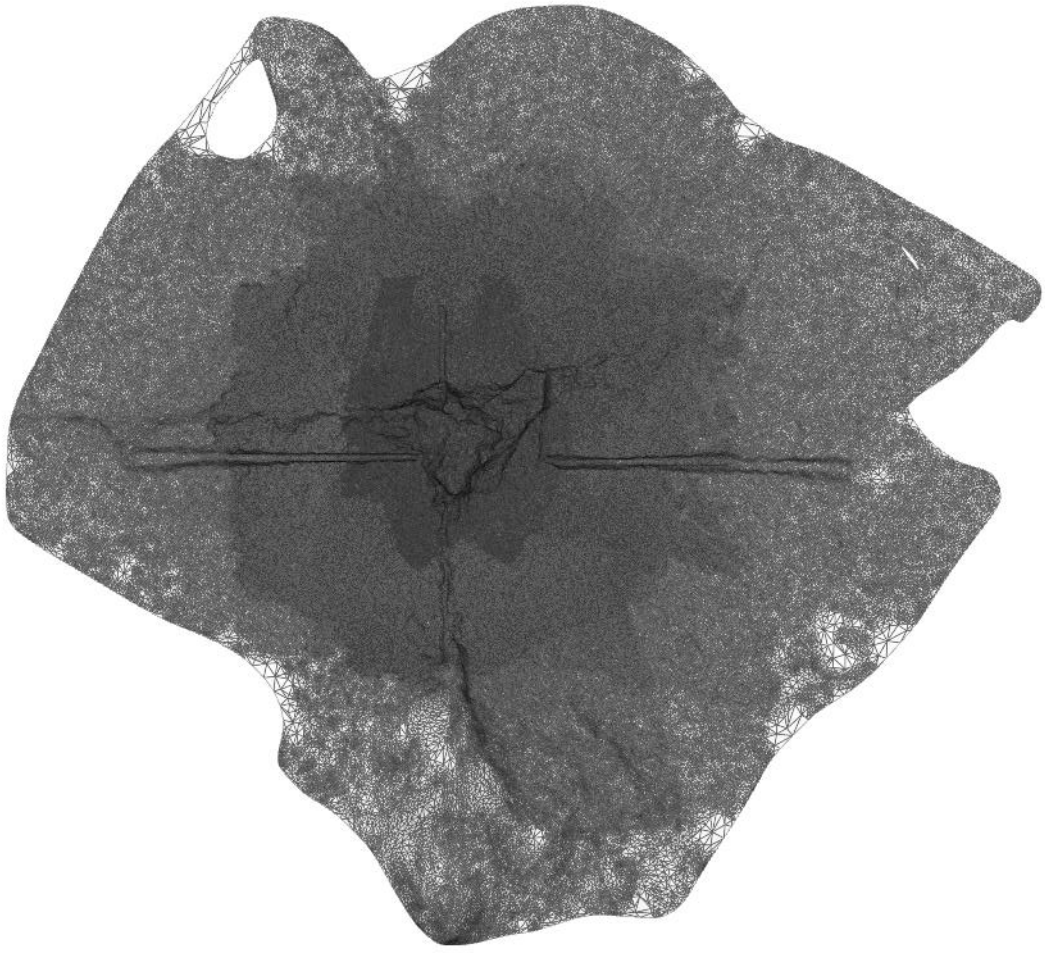

Figure 8 3D Model Produced Through Photogrammetry

1.3.6 Editing the Spall Model

Printing the entire model was time-consuming. To reduce this printing time, a cropping tool was used to reduce the spall model, as shown in Figure 9.

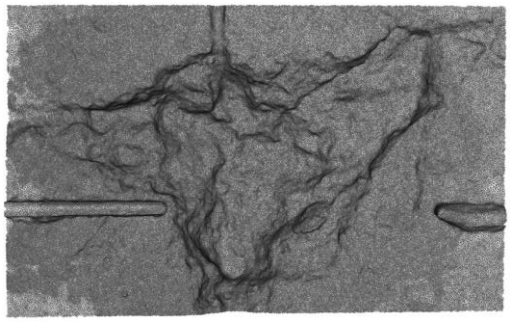

Figure 9 3D Scanned Spall

1.3.7 Modifying the 3D Model

The resulting 3D scanned model resembled an upside-downed cone, as shown in Figure 10; this was because only the surface of the spall was scanned. If this model was printed as is, the output would not have worked as a mold into which concrete could be poured and cured.

Figure 10 Shape of the 3D Scanned Model Produced Via Photogrammetry

The bottom of the printed form needed to be flat in order for it to be stable while the concrete was curing. Also, it was necessary that the edges the 3D scanned model have walls have to be the same depth as the depth of the spall. So, the extruded edges help to support until the fresh concrete is cured. Thus, the edges where are the highlighted parts of the 3D model needed to be extruded, as shown in Figure 11.

Figure 11 3D Model Modification

After this process, the modified 3D model was ready to be printed out as a concrete segment mold, as shown in Figure 12.

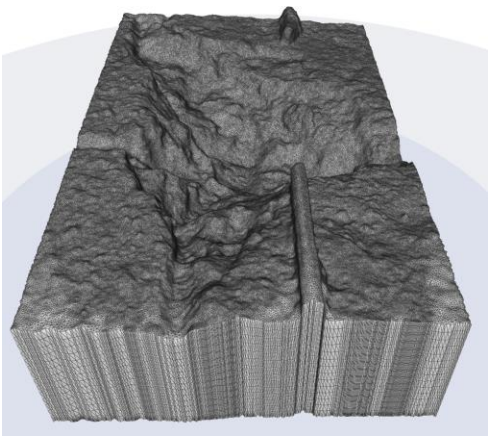

Figure 12 Modified 3D Model

However, it was also necessary to determine if any distortion existed in the final model, as well as if it was ready to be printed. If there were holes on top of the 3D model surface after the model was modified, the 3D printed model could not have been used as a mold. Thus, the errors of a 3D model should be fixed by the functions of Autodesk ReMake. Those errors can be detected and fixed automatically after the function is running. After that, the final model was checked manually by using another visualization function to check whether there are distortions as shown in Figure 13.

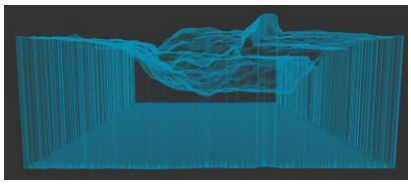

Figure 13 Checked Model

1.3.8 Using 3D Printer to Duplicate the Shape of the Spall Damage

A commercial fused deposition modeling type 3D printer was used to fabricate a duplicate of the spall, as shown in Figure 14. This prototype was employed as a form into which concrete was poured and cured; the result was a concrete segment.

Figure 14 3D Printed Mold for a Concrete Segment

1.3.9 Placing the Concrete

The concrete was then poured into the printed form and cured in a temperature and humidity controlled room; the high-quality concrete section that resulted was produced by minimizing the dry shrinkage and protecting the segment from infiltration by chemical substances, as shown in Figure 15.

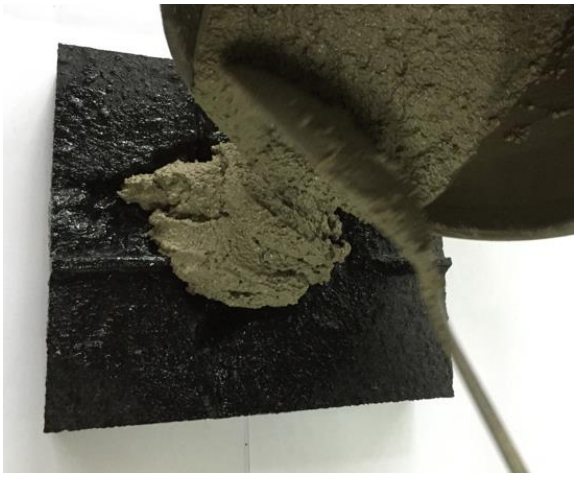

Figure 15 Placing the Concrete

1.3.10 Production of the Prefabricated Concrete Segment

A concrete segment was produced that would fit the spall (see Figure 16). Before the concrete was poured into the mold, form oil was spread inside; this allowed for easy removal. Also, the form oil helped prevent the fresh concrete from sticking to the mold while it was hardening.

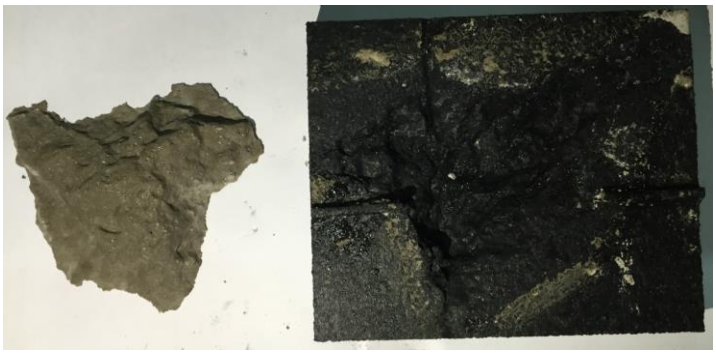

Figure 16 Concrete Segment

1.3.11 Gluing the Prefabricated Concrete Segment onto the Spall

Once the concrete was fully cured, it was removed from the form. Before the concrete segment was glued onto the spall, the contact area between the segment and the surface was cleaned; the goal was to remove all debris so that once they were fit together, the connection would be a tight one. An epoxy-resin adhesive was then applied to the damaged surface of the concrete (see Figure 17) and the concrete segment. Finally, the concrete section was inserted into the spall.

Figure 17 Applying Adhesive to the Concrete Segment

1.3.12 After Gluing the Prefabricated Concrete Segment onto the Spall

A spall is filled with a prefabricated concrete segment (see Figure 18). And the road can be reopened to let a vehicle passes over the repaired area. This was the last step in the spall repair sequence.

Figure 18 After Gluing the Prefabricated Concrete Segment onto the Spall

1.4 Research Question

Once the concrete segment generated by a 3D printed mold was glued onto a spall, the road can be reopened for use and vehicles passing over the repaired area applied vertical force to the concrete segment. It is important to note that the worst case applied stress generated by national standard weights (US DoT 2013) do not yet contain measurements for when a container truck continues to accelerate rapidly on the concrete segment or stops suddenly on top of the concrete segment. If the strength of the segment

was able to handle the vertical force generated by the vehicles and there were no elevation differences between the repaired and undamaged areas, the vertical force would not harm the repair. However, if the applied stresses were greater than the glue strength when the friction force generated by a container truck changing speeds was applied to the repaired area, the repair segment would be ejected. Conversely, if the strength of the concrete was greater than the stress generated inside the segment by the friction force of a tire of a container truck, the friction force would not destroy the concrete. Thus, the research question is that the attached prefabricated concrete segment is strong enough to handle the applied stress?

1.5 Research Objective

The objective of this research is to see if 3D scanning and printing technology can be used to repair spall damages to concrete pavement. More specifically, this work investigates the main stress flowing along the boundary of an oval-shaped concrete segment. As addressed above, it is reasonable to assume a certain amount of gap between the bottom of the concrete segment and the surface of a spall; in this study, that gap was filled by glue that, once hardened, had a certain amount of thickness. The method used to test the glue strength included a determination of the main stress, in order to mimic a vehicle traveling over the repaired area.

This research also investigated the stresses applied to a bonding interface when a tire spins on top of an attached concrete segment. To achieve the goal of this inquiry, a

finite element analysis was conducted to identify the primary tensions (among shear, compressive, and tensile stresses) resulting from a tire pressing on a glued concrete segment. The applied stresses were determined according to a single-axle 20,000 pound (9 ton) moving container truck, which was the national standard when the concrete road was designed (US DoT 2013).

Finally, this research examined the mathematical relationship between the glue thickness and the resisting force of the glued concrete segment against the shear strength applied to the glued layer, and verified this mathematical relationship through slant-shear tests.

1.6 Research Methodology

Empirical research is a method using evidence to obtain knowledge through direct and indirect observations or experiences (Ellysa 2015) and two forms of this method are quantitative and qualitative studies. Quantitative empirical research is a systematic investigation through the observation of phenomenon employing statistical, mathematical, or computational techniques (Lisa 2008). Qualitative research is a study in which people are invited to express their opinions on a subject through qualified and systematic questions used to gather information on the subject (Norman and Yvonna 2000). To test the structural sustainability of this suggested spall repair, a quantitative empirical research is used to analyze data from a shear strength test and the results are compared with the determined applied stress by a container truck.

2. LITERATURE REVIEW

2.1 Concrete Adhesives

Bonding agents are used to attach individual structural members together. Among the many available glue types, latex and epoxy resin-based bonding agents are two adhesives commonly used in the construction industry (Mailvaganam 1997). These glues are usually employed in repair applications to bond a new concrete structure to an old concrete substrate. They offer substantial strength and an outstanding level of waterproofing (Mailvaganam 1997). Thus, the bonding systems most widely used in the construction industry are latex emulsion and epoxy. The proper glue is a key to structural longevity, and thus essential to the spall repair method examined in this research. Hence, the proper adhesive had to be selected before the slant-shear test could be executed.

2.1.1 Latex Bonding Adhesive

Since this study filled a spall with a hardened concrete segment, the bonding agent needed to be very strong and able to bond hardened concrete to hardened concrete. It was determined that it would not be possible to use a latex bonding agent, because such adhesives are more appropriate for bonding fresh concrete to old concrete. There

are four main latex emulsion-based bonding applications in construction. The characteristics of each are described below (Mailvaganam 1997).

- Acrylic: This type of bonding system is used to bond fresh concrete to old concrete, and is appropriate for repairing both indoor and outdoor damage to steel, wood, or thin section toppings. This type of adhesive is ineffective in repairing damages due to extreme chemical exposure or high hydrostatic pressure.

- Polyvinyl – Acetate: This type of glue is usually applied to bond fresh concrete to old concrete and thin layer toppings. It is appropriate for applications involving indoor or outdoor damage to steel, wood, or thin section toppings, but improper for repairing harm resulting from extreme chemical exposure or high hydrostatic pressure. Additionally, it cannot be re-emulsified.

- Butadiene – Styrene: This bonding agent is usually applied to bond fresh concrete to an existing concrete structure or thin layer topping. It is appropriate for use in repairing either indoor or outdoor damage to steel, wood, or thin section toppings. However, it is inappropriate for use in extreme chemical exposure and high hydrostatic pressure-related repairs.

- Polyvinyl Acetate: This latex bonding agent is used to bond plaster, primarily on indoor ceilings. This adhesive is rarely used as a concrete bonding agent.

2.1.2 Epoxy Resin Bonding Adhesive

ASTM C881 / C881M-14, the standard specification for epoxy resin-based bonding systems for concrete, classifies these types of glues according to their intended use (ASTM C881 2015). Among the seven categories, Type IV is most often used as a bonding system for attaching concrete segments to one another. Detailed descriptions of the adhesive types are included below.

- Type I - (Non-Load Bearing Application): This type is used to bond hardened concrete to hardened concrete and other materials.

- Type II - (Non-Load Bearing Application): This type is most commonly used to bond freshly mixed concrete to hardened concrete.

- Type III: This is a skid-resistant bonding material for hardened concrete, often employed as a binder in the epoxy concrete used for traffic-bearing surfaces.

- Type IV - (Load-Bearing Application): This is frequently used to bond hardened concrete to hardened concrete and other materials, and as a binder for epoxy concrete.

- Type V - (Load-Bearing Application): This type is regularly employed to bond freshly-mixed concrete to hardened concrete.

- Type VI: This bonds and seals segmentally precast elements.

- Type VII - (Non-Stress Carrying Sealer): This is used for segmentally precast elements when temporary post-tensioning is not applied, as in a span-by-span erection.

2.2 Literature Review of Shear Strength Tests

Typical spall damage looks like a dent in the surface of a concrete structure. The size of the spall expands when chemical materials penetrate or there is an external impact (PCA 2001). Thus, a spall gets wider and becomes deeper if the initial damage is not repaired. Such flaws can cause structural problems and rebar corrosion inside the concrete. Therefore, they need to be repaired as quickly as possible (US DoT 2008). To fully repair damages to concrete and make it structurally sustainable, the material applied should have properties similar to those of the existing concrete substrate. At this point, any adhesion that is revealed once the concrete hardens will not be strong enough to attach to a spall. Thus, adhesion of concrete patches must be improved through the use of an epoxy adhesive. However, the current repair process has laborers randomly applying the glue, without following any specific criteria. If glue strength is impacted

by bond line thickness, then bond line thickness is one of the most important factors to consider when applying glue. However, since concrete is self-loaded, it is difficult to control bond line thickness. Because of this difficulty, there is no current research on how bond line thickness on concrete surfaces influences the strength of a glue.

The joint strength of a glue is influenced by various factors and depends upon the material properties of the bond; it is also influenced by the mechanical properties of the adherend, thickness of the adhesive layer, curing temperature of the glue, test method employed, and various interfacial harshness levels (Broughton and Gower, 2001). In addition, overlap length and bond line thickness influence the strength of the glue (Davies et al. 2009). The aerospace, automotive, and marine structure industries are all actively investigating the influence of bond line thickness. In aerospace, a stringer is used to attach the fuselage, while a metal honeycomb structure is employed to attach the empty wings; this prevents buckling during a flight (Gleich 2002). In the automotive field, boot lids and bonnets make noise when loosely attached. Therefore, they are fastened to the vehicle's mainframe with a bond in order to prevent clatter (Gleich 2002). When repairing a marine structure, engineers cut out the damage and bond on a new iron plate (Davies et al. 2009).

In the construction industry, adhesives are used in various ways, and there are a wide variety of factors that affect their effectiveness and user safety. Thus, numerous studies are actively investigating the factors influencing adhesive strength. Bonding agents are also widely used in the construction sector. A representative example is in spall repair on concrete roads; bonding agents improve the strength of the adhesion of

the concrete patching. Latex bonds are more suitable for indoor use, because they lack resistance to water and chemicals. Thus, epoxy resin bonds capable of resisting external environmental factors are used widely. However, research has yet to be conducted on the important factors affecting the strength of adhesives in other industries. Moreover, there is no standard recommended application amount, when applying epoxy resin glue to a concrete surface. If bond line thickness is an important factor affecting the strength of an adhesive, it is essential that it is considered when applying epoxy resin to a concrete surface. Since there is currently no research on whether or not bond line thickness influences a bond's strength when adhering to concrete, this study gives an overview of how the bond line of a section of concrete impacts the strength of a glue.

A number of studies have been conducted on the influence of bond line thickness on the shear strength of a glue. Bryant and Dukes (1967) examined the tendency of shear strength in response to changes in the thickness of an epoxy resin layer. Two types of epoxy resin were analyzed. To make the first, tetrabromobisphenol A was used as the epoxy and the slower-reacting aliphatic amines was applied as a hardener. The second glue was made with bisphenol A and an aliphatic amine hardener. Mild steel or aluminum alloy served as the adherend. To determine the shear strength of the epoxy resin, the researchers selected ASTM D1002-10 Single-Lap-Joint Adhesively Bonded Metal Specimens by Tension Loading (Metal to Metal). The thicknesses of the glue layers were controlled at 0.01mm, 0.013mm, 0.25mm, and 1.3mm, with various thicknesses of copper wire (Bryant and Dukes 1967).

Similarly, Chai (1993) evaluated whether or not various bond line thicknesses influenced the shear strengths of epoxy resin adhesives. Two types of glue were tested by the ASTM E229 Standard Test Method for Shear Strength and Shear Modulus of Structural Adhesives (Napkin Ring Shear Test). The first adhesive consisted of bisphenol A and an aromatic amine. A bisphenol A epoxy and hardener of latent aliphatic amine were used to make the second epoxy resin glue. To control bond line thickness, copper wire or glass fiber was used. The controlled thicknesses were: 5μm, 15μm, 35μm, 40μm, 100μm, 300μm, 500μm, 650μm, and 750μm (Chai et al. 1993).

Liang and Liechti (1996) used bisphenol A and amido amine to study the material properties of an epoxy resin glue. They controlled the bond line thickness at 0.254mm and determined the shear strength. The test method used was ASTM D 3518, which is a modified Arcan Test. The Arcan adherend material was an aluminum alloy (Liang and Liechti 1996).

Tomblin, Yang, and Harter (2001) tested three different adherends and four different bond line thicknesses via three different testing methods, identifying the shear strengths according to each variable. The study also highlights the relationship between shear stress and strain when a bond line thickness is changed. The tests were executed according to three test methods: ASTM D 1002 Standard Test Method for Apparent Shear Strength of Single-Lap-Joint Adhesively Bonded Metal Specimens by Tension Loading (Metal-to-Metal), ASTM D 3165 Standard Test Method for Strength Properties of Adhesives in Shear by Tension Loading of Single-Lap-Joint Laminated Assemblies, and ASTM D 5656 Standard Test Method for Thick-Adherend Metal Lap-Shear Joints

for Determination of the Stress-Strain Behavior of Adhesives in Shear by Tension Loading. Three epoxy resin adhesives were selected for analysis. Bisphenol A and epichlorohydrin were mixed to create the first glue, bisphenol A and aquatic acute 2 were combined for the second adhesive, and bisphenol A and epichlorohydrin copolymer were used as the third bonding agent. The adherend's materials were aluminum alloy, or carbon or E-glass fabric. The bond lines were controlled at 0.381mm, 1.016mm, 2.032mm, and 3.048mm. Finally, the shear strengths were determined according to four different bond line thicknesses (Tomblin et al. 2001).

Gleich (2002) used one epoxy resin bonding agent with bisphenol A and epichlorohydrin. ASTM D 1002 Standard Test Method for Apparent Shear Strength of Single-Lap-Joint Adhesively Bonded Metal Specimens by Tension Loading (Metal-to-Metal) was selected as the test method. The glue layer's thicknesses were controlled at: 0.1mm, 0.2mm, 0.5mm, 3mm, and 6mm (Gleich 2002).

In 2004, Chai conducted an additional study with bisphenol A as the epoxy and latent aliphatic amine as the hardener. The bond line thicknesses were 3μm, 6μm, 15μm, and 45μm and ASTM E229 Standard Test Method for Shear Strength and Shear Modulus of Structural Adhesives (Napkin Ring Shear Test) was selected as the test method (Chai 2004).

Jarry and Shenoi (2006) used a Butt Strap Shear Test, a modified ASTM D1002-10, to identify the shear strengths of a single epoxy resin glue (modified bisphenol A and aliphatic amines). The adherend was comprised of aluminum alloy, and the controlled bond line thicknesses were 1mm, 5mm, and 10mm (Jarry and Shenoi 2006).

Silva et al. (2009) tested the shear strengths of three epoxy resin glues – a very ductile polyurethane adhesive, extremely brittle two-component epoxy resin, and intermediate two-component epoxy cement – via ISO 11003-2 Adhesives: Determination of Shear Behavior of Structural Adhesives, Part 2: Tensile Test Method Using Thick Adherends. The material of the adherend was aluminum, and the bond line thicknesses were 0.5mm, 1mm, and 2mm (Silva et al. 2009).

Arena et al. (2010) determined the shear strength of a high viscosity acrylic adhesive (Henkel Loctite 330) through ASTM D1002-10 Single-Lap-Joint Adhesively Bonded Metal Specimens by Tension Loading (Metal to Metal). Bond line thicknesses were controlled from 0.4mm to 0.8mm (Arenas et al. 2010).

Davies et al. (2009) selected bisphenol A as the epoxy and trioxatridecane diamine as the hardener for making their epoxy resin glue. The controlled bond line thicknesses were 0.4mm, 0.5mm, 0.8mm, 1mm, and 1.15mm. The shear test method was an Arcan test, and the material of the adherend was aluminum (Davies et al. 2009).

Afendi (2011) used bisphenol A as the epoxy and a tertiary amine as the hardener for their bonding agent; the bond layers were controlled at: 0.1mm, 0.3mm, 0.6mm, 0.8mm, and 1.1mm. The shear test method was a Butt Strap Shear Test and the adherend's material was aluminum (Afendi 2011).

Aydin et al. (2012) used three epoxy resin glues (Devcon A, Devcon Titanium, and Akfix E300); the bond line thicknesses were controlled at: 0.1mm, 0.3mm, and 0.5mm. The Prismatic Plug-In Joints Shear Test, which is a modified ASTM D1002, was used to determine the shear strengths of the glues (Aydin et al. 2012).

Banea et al. (2015) selected a polyurethane adhesive and controlled the bond line thicknesses at: 0.2mm, 0.4mm, 0.6mm, 0.8mm, 1mm, and 2mm. The shear strength of the glue was determined through ASTM D 1002 Standard Test Method for Apparent Shear Strength of Single-Lap-Joint Adhesively Bonded Metal Specimens by Tension Loading (Metal-to-Metal) (Banea et al. 2015).

2.3 Test Results of Previous Works

Earlier studies on the relationship between bond line thickness and the shear stress of an epoxy resin bond layer all used steel as the adherend; their results are as follows. Bryant and Dukes (1967) employed two types of epoxy resin glue. The first used tetrabromo bisphenol A as an epoxy and a slower-reacting hardener; the second used bisphenol A as an epoxy and aliphatic amine as a hardener. The bond line thickness was controlled from 0.01mm to 1.3mm through the ASTM D1002 standard test method; the strength tended to decrease as the thickness of the bond layer increased. The average shear stress of the first glue was 1.45 MPa, and the average shear stress of the second glue was 13.24 MPa (Bryant and Dukes 1967). Chai (1993) attempted to determine the shear stresses of epoxy resin glues when the bond line thicknesses were controlled from 5μm to 750μm. The study analyzed two glues. The first used bisphenol A as the epoxy and aromatic amine as the hardener; the second used bisphenol A as the epoxy and latene aliphatic amine as the hardener. The test method was ASTM E229. As a result, the shear strength increased when the thickness of the bond layer was 0μm to

10μm, and the shear strength tended to decrease as the bond thickness increased above 10μm. The average shear strength of the first adhesive was approximately 110 MPa, and the average shear strength of the second adhesive was approximately 70 MPa. The relationship between the shear stress and strain of the epoxy resin increased without any deformation, until the strength reached the yield stress; when the strength exceeded the yield stress, it appeared deformed and entered the plastic region. This exemplified the trend experimentally identified in this study (Chai 1993). Liang and Liechti (1996) conducted experiments to determine the compressive, tensile, and shear stresses of one epoxy resin adhesive mixed with bisphenol A and amidoamine. The researchers controlled the bond line thickness at 0.254mm for the shear stress test. An Arcan test, also known as a modified ASTM D 3518, was selected to determine the shear stress; the test results showed 18.2 MPa (Liang and Liechti 1996). Tomblin et al. (2001) examined three epoxy resin adhesives: bisphenol A – epichlorohydrin, bisphenol A – aquatic acute 2, and bisphenol A – epichlorohydrin copolymer. The bond line thicknesses were controlled at 0.381mm, 1.016mm, 2.032mm, and 3.048mm. Three test methods were selected: ASTM D 1002, ASTM D 3165, and ASTM D 5656. With all of the bonds and in all of the test methods, the shear strengths tended to decrease as the bond layer thicknesses increased. Also, the average shear strengths of the ASTM 1002 and ASTM 3165 test methods were similar, and the average shear strengths of each bond were approximately 15 MPa, 11 MPa, and 14 MPa. The average shear strengths were approximately 36 MPa, 28 MPa, and 25 MPa when the tests were executed through ASTM 3165. This experiment proved that the test method matters as much as the

adhesive used (Tomblin et al. 2001). Gleich (2002) used ASTM D 1002 to examine the shear stress of an epoxy resin adhesive that used bisphenol A as an epoxy and epichlorohydrin as a hardener. The thicknesses of the bond line were adjusted to 0.1mm, 0.2mm, 0.5mm, 3mm, and 6mm. The shear strength of the bond line increased to 0.5mm, and decreased thereafter. The average shear strength was 10 MPa (Gleich 2002). Chai (2004) used ASTM E229 to test the relationship between bond line thickness and shear strength. The selected epoxy resin glue was mixed with bisphenol A and latent aliphatic amine, and the bond layer thicknesses were controlled at 3μm, 6μm, 15μm, and 45μm. The trend of this epoxy resin adhesive was found to decrease with the increasing thickness of the bond line. This meant that the shear strength of this bond was approximately 68 MPa (Chai 2004). Jarry and Shenoi (2006) controlled the bond line thicknesses of one of the modified epoxy resin glues that contained bisphenol A and aliphatic amines; the thicknesses were 1 mm, 5 mm, and 10 mm. The shear strength was measured by ASTM D1002-10 and the results showed that the shear strength decreased as the bond line thickness increased. The mean shear strength of the bond was about 9 MPa (Jarry and Shenoi 2006). Silva et al. (2009) used three epoxy resin glues, a very ductile polyurethane adhesive, a very brittle two-component epoxy adhesive, and an intermediate two-component epoxy adhesive. The controlled bond line thicknesses were 0.5mm, 1mm, and 2mm, and the shear strength of the epoxy resin glue was measured by ISO 11003-2. The tendency of the shear strength was found to decrease as the bond line thickness increased. The average shear strengths were approximately 30 MPa, 18 MPa, and 8 MPa (Silva et al. 2009). Arena et al. (2010) conducted a shear strength test using a

high viscosity acrylic adhesive. The test method was ASTM D1002-10. The shear strength was determined when the thickness of the bond line increased from 0.1mm to 0.8mm. The test results showed that the shear strength increased to 0.3mm and decreased after 0.3mm. The average shear strength of this bond was approximately 6 MPa (Arenas et al. 2010). Davies et al. (2009) constructed 0.4 mm, 0.5 mm, 0.8 mm, 1 mm, and 1.15 mm bond line thicknesses with epoxy resin glue that mixed bisphenol A and trioxa tridecane diamine. The test method was an Arcan test used to determine shear strength. As a result, the shear strength decreased when the bond line thickness increased (Davies et al. 2009). Afendi (2011) controlled the thickness of the bond line at 0.1mm, 0.3mm, 0.6mm, 0.8mm, and 1.1mm when using an epoxy of bisphenol A and a tertiary amine resin adhesive. The trend of changes in the shear strength was investigated through a butt strap shear test. As a result, the shear strength tended to decrease when the bond line thickness increased (Afendi 2011). Aydin et al. (2012) used three commercial epoxy resin adhesives, Devcon A, Devcon Titanium, and Akfix E300, to form bond line thicknesses of 0.1mm, 0.3mm, and 0.5mm, respectively. An ASTM D1002 standard test method was used to identify the shear strengths. As a result of the experiment, the thinnest bond line developed the highest shear strength. The average shear strengths of the bonds were approximately 3.5 MPa, 2.9 MPa, and 2.2 MPa (Aydin et al. 2012). Banea et al. (2015) measured shear strength by adjusting the bond layer thicknesses of a polyurethane adhesive to be 0.2mm, 0.4mm, 0.6mm, 0.8mm, 1mm and 2mm. Shear strength was measured by ASTM D 1002; the shear strength decreased as the bond line thickness increased. The average shear strength was 20 MPa

(Banea et al. 2015). This study used bisphenol A, a typical epoxy material. The bisphenol A was mixed by using three different types of resins – a modified aliphatic amine, modified cycloaliphatic amine, and modified aromatic amine – to make three different epoxy resin glues. The average maximum shear stresses were 12.02 MPa, 13.59 MPa, and 15.29 MPa, and the average yield stresses were 10.91 MPa, 12.58 MPa, and 14.49 MPa, respectively.

2.4 Summary of Previous Works

A summary of the previous studies on the impact of bond line thickness on bond shear strength is as follows. First of all, the thickness of the bond affects the shear strength of the glue. As the bond line becomes thicker, the shear strength tends to decrease. As the bond thickness decreases, the intensity of the shearing strength increases, and then decreases after reaching maximum intensity. Davies (2009) attempted to identify the elements affecting bond line thickness and the strength of a glue through a refined experiment involving Raman spectroscopy and nanoindentation. However, the impact of bond line thickness on the shear strength of epoxy resin glue has yet to be determined (Davies et al. 2009).

2.5 Literature Review of 3D Scanning and Printing Technologies Used for Restoration

2.5.1 Dental Prostheses Using 3D Scanning and Printing Technologies for Restoration

Dental problems cause pain and disrupt people's lives. Currently, dentists are studying ways of integrating existing treatment methods with emerging technologies in order to facilitate quick recoveries and reduce costs. Mormann and Bindl (1996) studied the applicability of 3D scanning and printing to the restoration of tooth damage. They found that emerging technologies could be used to treat damaged teeth faster and more accurately than current practices (Mormann and Bindl 1996). Liu (2005) provided an overview of 3D scanning and printing integrated with dental prostheses, and discussed operational components, methodologies, and restorative materials that could be applied (Liu 2005). Williams et al. (2006) used 3D scanning and printing to create dentures, minimizing patients' inconvenience and creating more precise prosthetics (see Figure 19). The researchers were able to successfully print out elaborate dentures in a very short period of time. (Williams 2006)

Fuster-Torres et al. (2009) studied how to apply 3D scanning and printing technologies to implant dentistry, emphasizing implant abutments and the manufacture of surgical templates to achieve implants that can be immediately applied (Fuster-Torres et al. 2009). Noort (2012) discussed the possibility of integrating this technology into advanced dental medicine, in order to improve treatment speed, reliability, and accuracy (Noort 2012). Kasparova et al. (2013) compared the quality of 3D-printed plaster dental casts and traditional plaster casts to determine if the former could replace the later. The

results showed that the 3D printed casts could serve as a substitute, resulting in better accuracy and lower prices (Kasparova, et al. 2013).

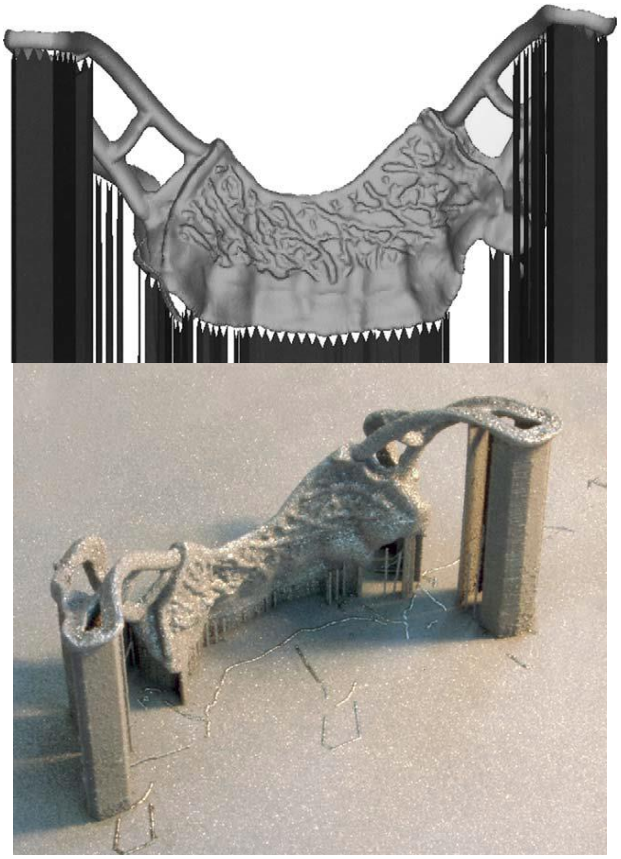

Figure 19 3D Model and Printed Denture (Williams et al. 2006)

2.5.2 Auricular Prosthesis for Restoration Using 3D Scanning and Printing Technologies

An auricular prosthesis can be used to restore external ears on people who have lost them due to injury or illness. External ear restoration is not easy, because the surgery requires an anaplastologist's assistance and complex instrumentation. Until now, significant time and money had to be spent to restore an external ear to be similar to the

ear on the opposite side of the patient's head. Studies are currently underway, however, that examine the application of 3D scanning and printing technology to restoring such ears at a much lower cost and in a significantly shorter amount of time. Ciocca and Scotti (2005) used a 3D laser scanner to mirror the undamaged ear, then printed out a model with a 3D printer; a cast was then manufactured for curing a wax ear that could serve as a prosthesis. The results indicated that even with the cost of the technology, the process would be both cost and time effective (Ciocca and Scotti 2004). Similarly, Liaxoras et al. (2010) showed that ears could be successfully restored using 3D scanning and printing. However, one clear difference was that Laxoras used a 3D scanning model acquisition system with five cameras and projectors, in order to create a more accurate 3D model (Liacouras et al. 2010).

Ciocca et al. (2006) studied how to make an implantable maxillofacial prosthesis through 3D scanning and printing. Since the optimal location for the implant could be determined before the cast was printed out, the results indicated that doctors would no longer need to cause the patient further discomfort by discovering the best positioning (Ciocca et al. 2006).

Ciobanu et al. (2013) also studied the creation of a prosthetic ear with a 3D printer; they used a structured light-scanning technique and a single camera stereo photogrammetric scanning method to determine a more cost-effective system than which had been used in earlier studies (expensive 3D laser scanners). This research explained how to get a high-quality 3D model with a more cost-effective 3D scanning technology (Ciobanu et al. 2013). He et al. (2014) also suggested a restoration procedure for the

external ear that employed a more cost-effective 3D printer. Since 3D scanning and printing technologies are expensive to set up, using cost-effective strategies are key to reducing the overall price of auricular prosthesis procedures (as shown in Figure 20). The results if that research indicated that the cost could be greatly reduced (He et al. 2014).

Finally, Jin et al. (2015) studied how to reduce 3D printing time through a parallel-based path generation method. The conclusion indicated that 3D printing time could be reduced, and the outcomes would result in more sophisticated surfaces (Jin et al. 2015).

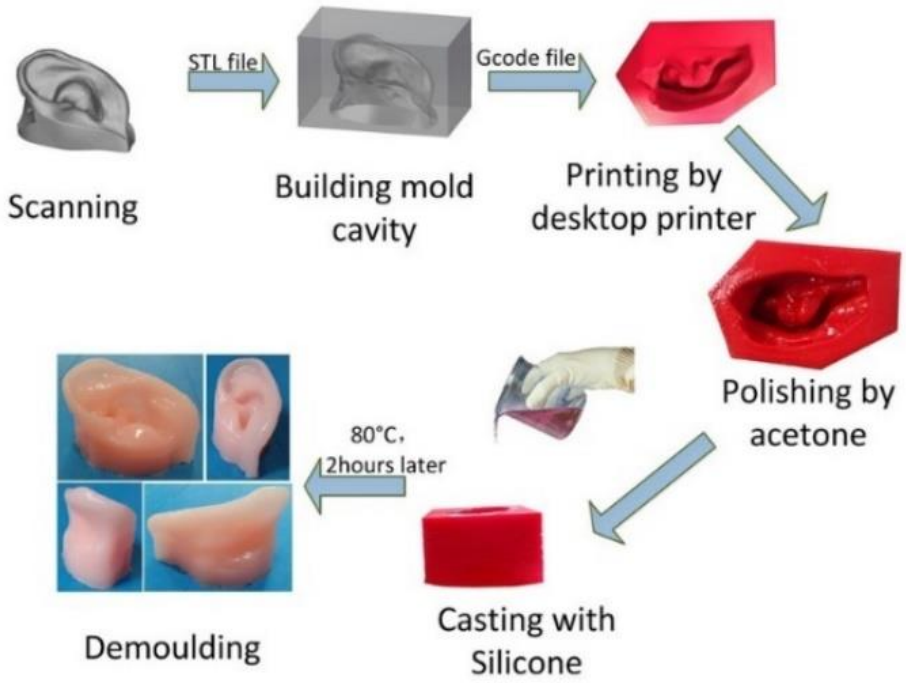

Figure 20 External Ear Restoration Procedure (He et al. 2014)

2.5.3 Historical Building Restoration Using 3D Scanning and Printing Technologies

Many historical buildings and statues have been destroyed or damaged during the wars that have recently plagued the Middle East. Three-dimensional scanning and printing have been applied to restoring these historical treasures. In cases of damage to symmetrical structures, the restoration team was able to scan the undamaged side and print out a patch or replacement with a powder-based 3D printer, as shown in Figure 21 (Scott 2016).

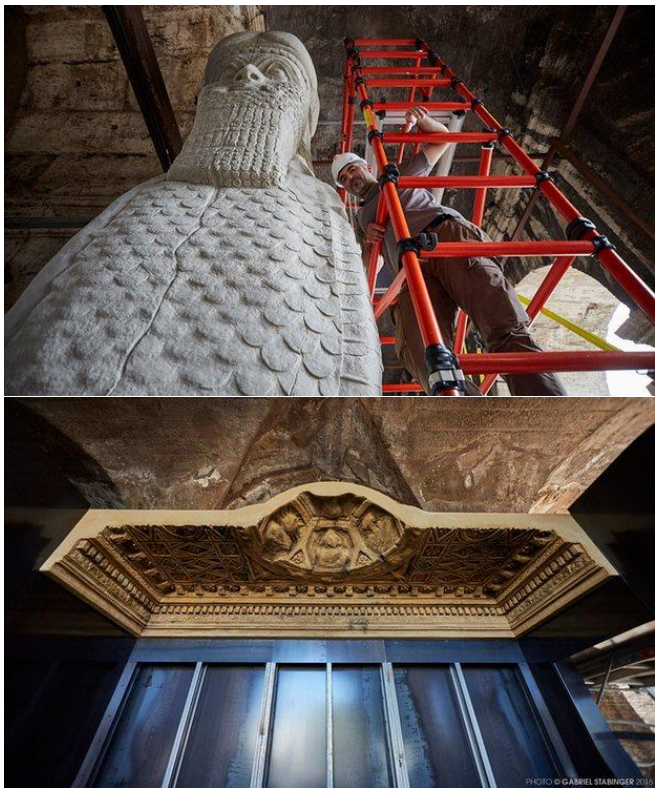

Figure 21 Restored Statue and Temple Ceiling (Scott 2016)

3. EXPERIMENT DESIGN

3.1 Laboratory Test

The most effective evaluation of the spall repair method addressed in this study would have been a long-term observation of a repair applied to an oval-shaped area of damage on actual construction. However, it is problematic to evaluate this new method when it is applied to actual spalls; the time required for long-term observation is a substantial issue. Moreover, at the time of testing it was not yet known whether the glue would be strong enough to handle the applied stress resulting from when a concrete segment is glued onto a spall (see Figure 22). Thus, laboratory tests were substituted for field tests, so that the evaluation could be completed in a timely and safety-conscious manner.

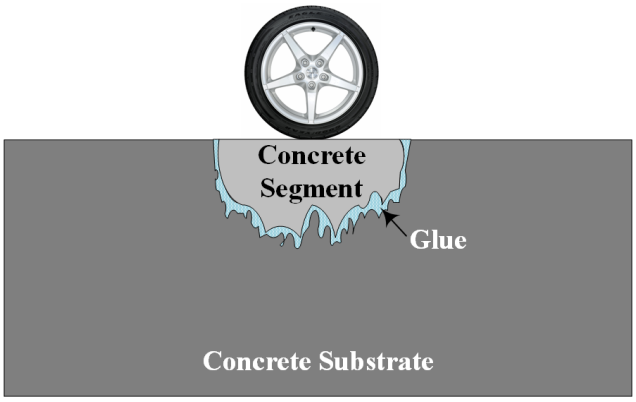

Figure 22 Applied Stress on a Spall

3.2 Simplification of Damaged Section

The damaged surfaces of concrete roads can take all different sorts of shapes. For convenience, this study simplified the shape of the test spall to be an oval-shaped bowl, as shown in Figure 23.

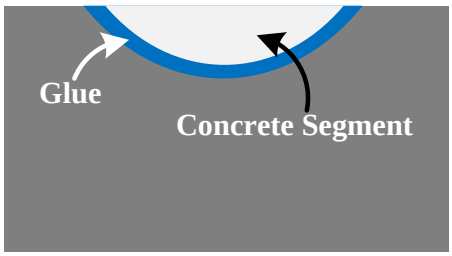

Figure 23 Simplified Spall Section

3.3 Finite Element Analysis

If the concrete segment was glued onto the spall and remained there without any applied stresses, it would probably not change. However, when a car passes over the patch, something causes the glue layer to drop away, but that action-reaction mechanism cannot be observed because the concrete is opaque. A simple finite element analysis was performed with ABAQUS to determine what happens along the bond line and determine the major stress that occurs when a car begins to move forward on a patch of this type. This analysis assumed that the glued concrete segment was a perfect fit for the spall, and the car began to accelerate once on top of it (as shown in Figure 24).

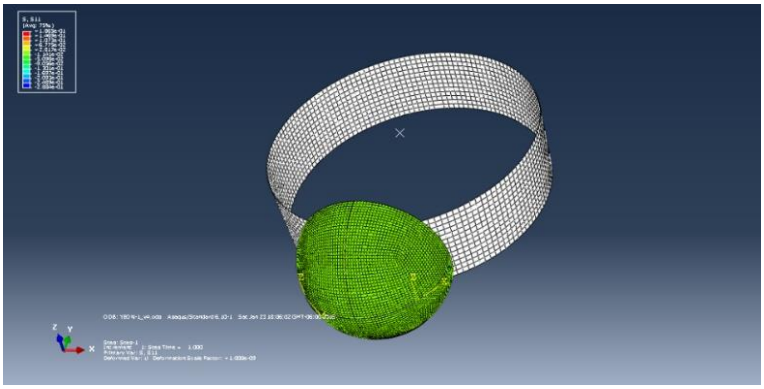

Figure 24 Stress Distribution when a Vehicle Moves on a Concrete Segment

Even though the shape of the concrete segment model was symmetrical, the reactions on the interface differed between the left and right slopes; this was because the tire of the vehicle was rolling on the concrete segment from left to right. It would have been nearly impossible to select the exact center node of each slope, because there were so many. Node 16, randomly selected in the middle of the left slope, and node 12, randomly selected in the middle of the right slope, appeared to be representative of the approximate center of each. The calculated major shear stresses for both sides are shown in Figure 25 and Figure 26.

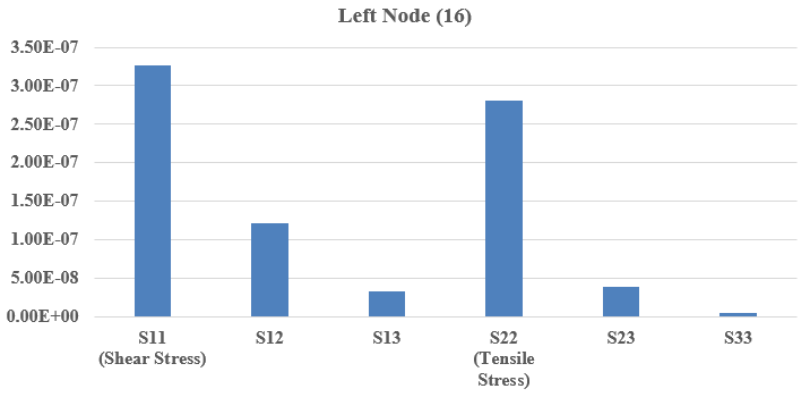

Figure 25 Major Stress of Left Side Along the Bond Layer (Unit: Von Mises)

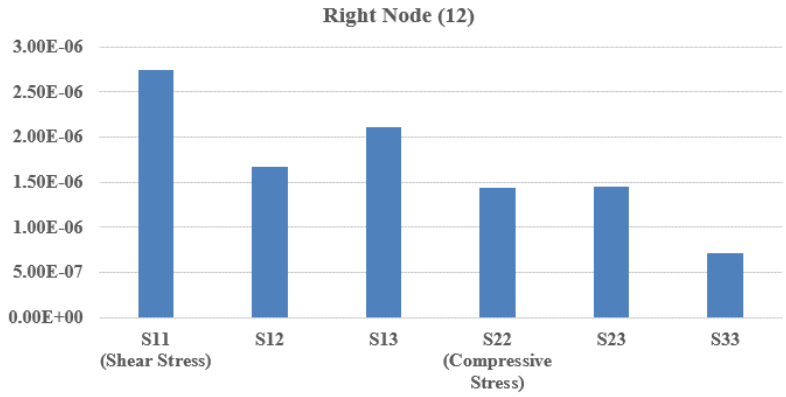

Figure 26 Major Stress of Right Side Along the Bond Layer (Unit: Von Mises)

The finite element analysis results indicated that shear stress was the major stress exerted when the car accelerated over the patch. Before the adhesive strength test began, the finite element analysis was necessary to discover out what is the major stress to determine the appropriate test method regarding the adhesive. As a result of the finite element analysis, this was found that a standard test method for the shear strength of the adhesive should be selected.

3.4 Breakdown of the Action-Reaction Mechanism

To understand the action-reaction relationship resulting from when a car accelerates above this type of patch, the significant elements needed to be determined and examined. First, because the maximum weight of a container truck is a national standard, the mass of a single-axis container truck was identified as an important factor (US DoT 2013). Second, a tire can begin to roll on top of a concrete patch at varying degrees of acceleration. Newton's second law was used to calculate the level of the

applied loadings, which are delivered by friction to the repaired area. This tension can reach the hardened glue layer, break it up, and even cause additional damage. To determine if the segment would bear up under the applied loads, two main factors needed to be considered: (1) how the shear strength of the glue would react to the applied force, and (2) if the weight of the concrete segment would be sufficient to resist the applied load. In the test case used for this research, these two components reacted to the applied force to keep the patch on the spall. The action-reaction mechanism is broken down and illustrated in Figure 27.

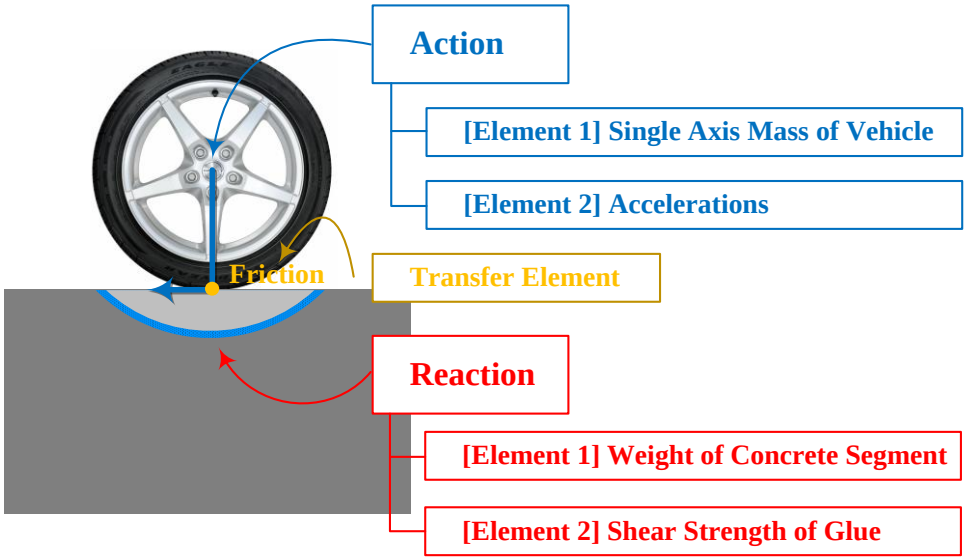

Figure 27 Breakdown of the Action-Reaction Mechanism

3.5 The Glue Layer

Photogrammetry was used to replicate the damage and create a 3D model, which was then input into a 3D printer to produce a mold for the fresh concrete.

In this study, an iPhone 6 (8 megapixels) was used to take the photos, in order to simulate an actual field application. By using this method, construction crews will be able to develop 3D models without using bulky devices such as 3D laser scanners; moreover, they will not require specific training (as they would with a scanner). In this research, a Fused Deposition Model-based 3D printer was used to produce the 3D mold. This 3D printer is one of the most common on the market, and is considered affordable.

It is important to remember that emerging techniques (such as the method described in this research) have tolerances that are caused by the limitations of current technology. The tolerance of photogrammetry depends upon camera resolution, scale control, and the number of photographs taken (Gonzalez-Jorge 2012). The tolerance of a 3D printer occurs when the fusing filament cools and contracts (Hernanadez 2015). Hence, the volume of the concrete segment was smaller than the volume of the spall it repaired; the glue had to fill the gap generated by both tolerances, as shown in Figure 28.

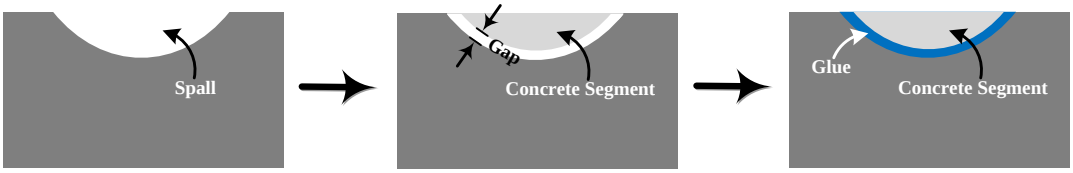

Figure 28 Orientation of the Glue Layer

4. ACTION: HOW STRONG WILL THE APPLIED STRESSES BE?

If the adhesive strength can handle the worst case of the applied stress, there would be no problem. Thus, the applied stress of the worst case should be determined. The worst case could be assumed this case the container truck stops on the concrete patch suddenly. When a 9-ton container truck suddenly stops, the spinning of the wheels stops at the same time. At this time, the wheels of the container truck slip a certain distance with drawing the skid marks. And then the vehicle stops. This skid mark can be explained by the friction between the tire and the concrete surface in physics. Let's take a look how strong will be applied stresses be by the friction force?

4.1 Applied Force

First, it is necessary to examine the vertical force of the vehicle. The vertical force can be defined as shown below.

$$N = mg$$

(where, N is vertical force, m is mass, and g is gravity)

Also, the frictional force can be defined regarding the vertical force when the vehicle suddenly stops as shown below.

$$f = \mu N = \mu mg$$

(where, f is frictional force, μ is coefficient of friction)

Basically, force is defined with the Newson's second law (F = ma). Also, the deceleration of the vehicle can be defined when a car stops as shown below.

$$f = F$$

or

$$\mu mg = ma$$

For this study, the friction coefficient between the surface of the tire and the surface of the dry concrete pavement was 0.8 (Bobo 2003). With this assumption, the deceleration of the vehicle can be determined following equation. This deceleration acts in a direction opposite to the traveling direction of the vehicle. Thus, the deceleration can be presented as:

$$a = \mu g = 0.8 \times (-9.8\, m/s^2) = -7.84\, m/s^2$$

(where, a is deceleration, μ is friction coefficient, and g is gravitational acceleration)

The applied stress was derived based on the federal maximum single-axle standard. The single-axle mass of the federal standard is 20,000 pounds (about m =

9,000kg) (US DoT 2013). Thus, the frictional force that applied on the concrete patch can be defined when the vehicle has stopped suddenly as shown below.

$$f = 9000\ kg \times (-7.84\ m/s^2) = -70{,}560\ N$$

4.2 Spall Areas

Stress is the force across the unit area. In other words, areas where forces are applied influence the degree of stress. Hence, a proper definition of the area is essential to accurately determine the stress. It is almost impossible to define the area of a spall because the size can vary greatly. US DOT defines the severity of a spall by its width, as shown in Figure 29 (US DoT 2003). This study used US DOT's degrees of damage to define the spall area. And the areas are assumed as a circle. The area was then divided by the applied force to determine the applied stress under a variety of accelerations.

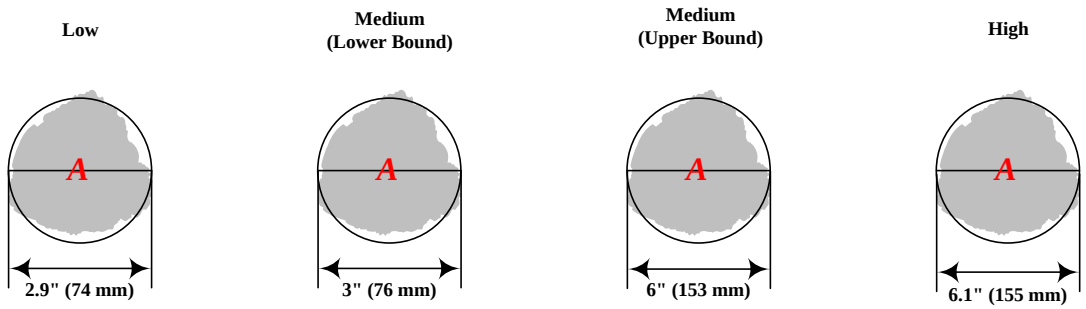

Figure 29 Spall Severity by Area

4.3 Applied Stresses

In this research, the applied stresses were the forces across the spall area when the vehicle suddenly stops and the vehicle moves forward on the concrete patch as shown below.

$$\sigma = \frac{f}{A}$$

When this friction force is applied to the concrete patch, the magnitudes of the applied stresses are shown in the following Table 2.

Table 2 Applied Shear Stress by Container Truck

Low (4,301 mm^2)	Medium - Low (4,537 mm^2)	Medium - Upper (18,386 mm^2)	High (18,870 mm^2)
16.41 MPa	15.55 MPa	3.84 MPa	3.74 MPa

The stress values calculated above are same as the applied stresses that the vehicle begins to move forward on the concrete patch. Also, a maximum shear stress of 16.41 MPa is applied to the concrete patch surface and this shear stress is delivered to the bottom of the concrete patch. Thus, if the adhesive is able to withstand the applied stress (16.41 MPa), it can be assumed that the concrete patch may remain stuck without falling off the spall.

5. REACTION: IS THE GLUED CONCRETE SEGMENT STRONG ENOUGH?

This chapter addresses whether or not the attached concrete segment is strong enough to be considered structurally sustainable. The spall repair method proposed here completes the repair process by applying an adhesive to the top of the spall to attach the concrete segment. Generally, this adhesive is resistant to loading and maintains structural stability. However, the weight of the concrete was chosen as one of the resistance factors because it would take a certain amount of loading to eject the concrete segment from the spall. Thus, two important elements of the reaction are the weight of the concrete and the shear strength of the bonding agent.

5.1 Weight of the Spall

Weight is generated when the mass of an object is held down by gravity, which is a downward force. In this research, the concrete segment's mass was held down by a downward force (see Figure 30). Friction develops between the contact area of the tire and the surface of the concrete segment. A load produced by a container truck delivered to the concrete segment through friction could force the segment out of the spall when the vehicle began to move forward or stopped suddenly.

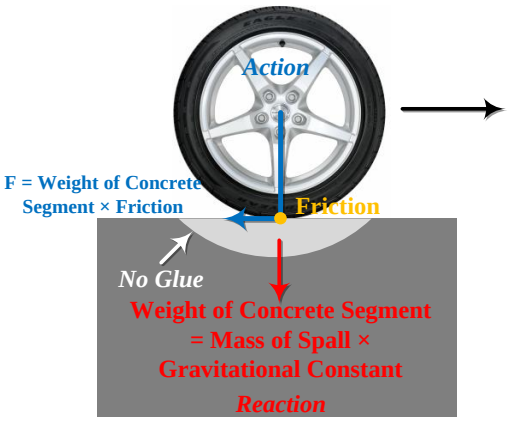

Figure 30 Concrete Segment on a Spall - No Glue

If there is no glue between the concrete segment and the spall, the concrete segment will slip out when the applied force is stronger than the weight of the segment (see Figure 31). In contrast, if the applied force is not stronger than the weight of the spall, the concrete segment will remain in place. This means that the weight of the concrete segment should be considered one of the reaction elements providing resistance to loadings. Thus, in this research the weight of the concrete segment needed to be determined, but only for the stresses applied to the glue layer.

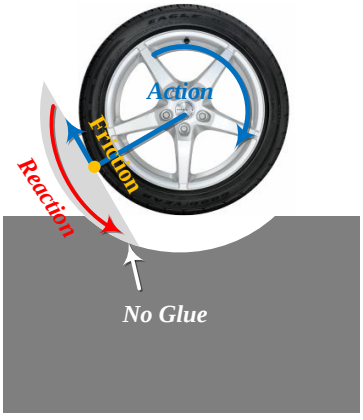

Figure 31 Slipping Concrete Segment

It is necessary to know how strong will the force will be to lift the concrete segment (see Figure 32). At this time, when the concrete segment is lifted, it is assumed that there is no friction between the bottom of the concrete segment and the surface of the spall. Also, since the concrete segment had stayed in the spall, there is no acceleration associated with the segment. In addition, the net force (F_{net}) is defined as the sum of all forces acting on an object. Applying this definition in this case, the net force must equal the mass times acceleration because the concrete segment stayed in the spall. It can be described mathematically as shown below.

$$F_{net} = ma$$

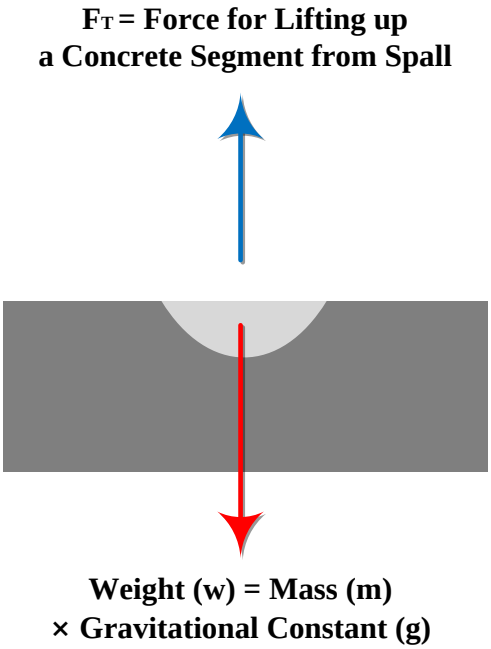

Figure 32 Force for Lifting a Concrete Segment from a Spall

Moreover, the lifting force can be explained as mathematically follows:

$$F_T - w = F_{net}$$

$$F_T - mg = ma$$

$$F_T - mg = m(0)$$

$$F_T - mg = 0$$

$$F_T = mg$$

(where, F_{net} is net force, F_T is the lifting force, w is weight)

As a result, the lifting force can be expressed mathematically, simply the mass times the gravitational constant.

5.1.1 Volume of the Spall

Basically, weight can be expressed as the volume of the object times the unit weight of the material. Thus, for this research the volume of the concrete segment needed to be identified in order to determine its weight. The volume of a spall is assumed to be a hemisphere for the convenience of calculation as shown in Figure 33.

To determine the volumes of a segments, the diameters of the hemisphere needs to be classified. To classify the diameters of the hemisphere, the longitudinal length of the spall was derived from data on spall severity provided by US DOT as shown in Table 3 (US DoT 2003).

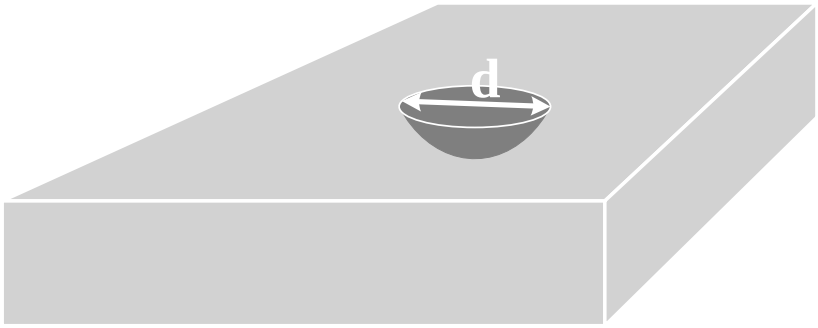

Figure 33 Volume of a Spall Assumed to be a Hemisphere

Table 3 Level of Spall Severity Classified by US DOT (US DoT 2003)

Severity	Low	Medium (Lower Bound)	Medium (Upper Bound)	High
Diameter (d)	74 mm	76 mm	153 mm	155 mm
Radius (r)	37 mm	38 mm	76.5 mm	77.5 mm

Based on the data, a volume of a hemisphere by severity of a spall can be determined as follows:

- Severity Low

Hemisphere Volume: $\frac{2}{3} \times \pi \times 37^3 = 106{,}034\ mm^3 = 0.000{,}106{,}034\ m^3$

- Severity Medium (Lower Bound)

$$\text{Hemisphere Volume: } \frac{2}{3} \times \pi \times 38^3 = 114{,}866\ mm^3 = 0.000{,}114{,}866\ m^3$$

- Severity Medium (Upper Bound)

$$\text{Hemisphere Volume: } \frac{2}{3} \times \pi \times 76.5^3 = 937{,}179\ mm^3 = 0.000{,}937{,}179\ m^3$$

- Severity High

$$\text{Hemisphere Volume: } \frac{2}{3} \times \pi \times 77.5^3 = 974{,}414\ mm^3 = 0.000{,}974{,}414\ m^3$$

5.1.2 Resistance Force by the Weight of the Spall

After the volume was calculated, the unit mass of the concrete ($2{,}300 kg/m^3$) was multiplied to determine the mass of the concrete segment as follows:

- Severity Low

$$\text{Hemisphere Volume} \times \text{Unit Mass} = 0.000{,}106{,}034\ m^3 \times 2{,}300\ \ kg/m^3 = 0.25\ kg$$

- Severity Medium (Lower Bound)

Hemisphere Volume × Unit Mass $= 0.000{,}114{,}866\ m^3 \times 2{,}300\ \ kg/m^3 = 0.27kg$

- Severity Medium (Upper Bound)

Hemisphere Volume × Unit Mass $= 0.000{,}937{,}179\ m^3 \times 2{,}300\ \ kg/m^3 = 2.16\ kg$

- Severity High

Hemisphere Volume × Unit Mass $= 0.000{,}974{,}414\ m^3 \times 2{,}300\ \ kg/m^3 = 2.25\ kg$

The mass is multiplied by the gravitational constant ($9.8\ m/s^2$) to determine the weight. The results of the weights of the spalls obtained are as follows:

- Severity Low

Hemisphere Mass × Gravitational Constant = $0.25\text{kg} \times 9.8\,\text{m/s}^2 = 2.45\text{kg} \cdot \text{m/s}^2$

- Severity Medium (Lower Bound)

Hemisphere Mass × Gravitational Constant = $0.27\text{kg} \times 9.8\,\text{m/s}^2 = 2.65\text{kg} \cdot \text{m/s}^2$

- Severity Medium (Upper Bound)

Hemisphere Mass × Gravitational Constant = $2.16\text{kg} \times 9.8\,\text{m/s}^2 = 21.17\text{kg} \cdot \text{m/s}^2$

- Severity High

Hemisphere Mass × Gravitational Constant = $2.25\text{kg} \times 9.8\,\text{m/s}^2 = 22.05\text{kg} \cdot \text{m/s}^2$

Here, the unit $\text{kg} \cdot \text{m/s}^2$ is the same as N. Therefore, the value obtained can be used as it is after switching the unit from $\text{kg} \cdot \text{m/s}^2$ to N as shown in Table 4.

Table 4 Lifting Force by Severity

Severity	Low	Medium (Lower Bound)	Medium (Upper Bound)	High
Lifting Force	2.45 N	2.65 N	21.17 N	22.05 N

5.1.3 The Applied Forces Along the Bond Layer

The obtained lifting forces are the magnitudes of the resistance forces by the weight of the concrete segment. Hence, after the resistance forces by the weight of a concrete segment are deducted from the applied forces produced by a container truck, the applied stresses only along the bond layer can be determined. The calculated results are shown in Table 5.

Table 5 Applied Forces Along the Bond Line

Severity	Low	Medium - Low	Medium - Upper	High
Applied force by a container truck	70,560 N	70,560 N	70,560 N	70,560 N
Resistance force by the weight of a concrete segment	2.45 N	2.65 N	21.17 N	22.05 N
Applied force along the bond layer	70,557.55 N	70,557.35 N	70,538.83 N	70,537.95 N

Also, after the calculated applied forces are divided by the area of the spall, the applied stresses along the bond layer can be determined as follows:

- Severity Low

$$\text{Applied Force along the Bond Layer} \div \text{Area of Spall}$$

$$= 70{,}557.55 \text{ N} \div 4{,}301 \text{ mm}^2 = 16.40 \text{ N/mm}^2 = 16.40 \text{ MPa}$$

- Severity Medium (Lower Bound)

$$\text{Applied Force along the Bond Layer} \div \text{Area of Spall}$$

$$= 70{,}557.35 \text{ N} \div 4{,}537 \text{ mm}^2 = 15.55 \text{ N/mm}^2 = 15.55 \text{ MPa}$$

- Severity Medium (Upper Bound)

$$\text{Applied Force along the Bond Layer} \div \text{Area of Spall}$$

$$= 70{,}538.83\ \text{N} \div 18{,}386\ \text{mm}^2 = 3.84\ \text{N/mm}^2 = 3.84\ \text{MPa}$$

- Severity High

$$\text{Applied Force along the Bond Layer} \div \text{Area of Spall}$$

$$= 70{,}537.95\ \text{N} \div 18{,}870\ \text{mm}^2 = 3.74\ \text{N/mm}^2 = 3.74\ \text{MPa}$$

5.1.4 Results after Removing the Spall Weights from the Applied Force

The final calculated results are shown in Table 6. After the results of this calculation, the weight of the concrete segment was not a major resistance element. Hence, with the proposed repair method, the shear strength of the glue was the most important structural-sustainability factor in handling applied stresses. Therefore, the applied stresses along the bond layer will be compared with the test results of the adhesive strength later.

Table 6 Applied Stresses Along the Bond Line

Severity	Low (4,301 mm^2)	Medium - Low (4,537 mm^2)	Medium - Upper (18,386 mm^2)	High (18,870 mm^2)
Stress	16.40 MPa	15.55 MPa	3.84 MPa	3.74 MPa

5.2 Shear Strength of the Glue

The proposed spall repair sequence begins by obtaining a 3D model through photogrammetry. Then it is printed out using a 3D printer. The output is used as a form to cure fresh concrete to be used as a patch on the spall. Each step of the spall repair sequence that is suggested in this study has its own possibility of error such as the level of the accuracy of the 3D scanner and the shrinkage of the outcome of the 3D printer. When these errors accumulate, we can simply assume that there will be a certain space between the bottom of the concrete segment and the surface of the damaged area when the concrete segment is later inserted into the spall. This space will be filled with an adhesive, and it is not yet known to what extent the adhesive layer will be formed. However, it can be predicted that the thickness of the adhesive layer will have some effect on how it will hold the concrete segment.

Also, through a finite element analysis, the identified major stress was the shear stress when a container truck accelerates or stops on the attached concrete patch. So, it could be a test method that can investigate the shear strength of the adhesives.

To sum up, the test method must be the shear strength test of the adhesives associated with the bond layer thickness between concrete adherend and concrete adherend.

5.2.1 Test Method for Determining Shear Stress

The standard test method (BS EN 12615) was selected to determine the shear strength of the epoxy resin adhesive applied to the concrete specimen (BS EN 12615 1999). BS EN stands for British Standard European Norm, also known as the British test standard. This standard method is used worldwide as an international standard, similar to the American Society Testing and Material (ASTM) system. BS EN 12615 is similar to ASTM C882 / C882M, also known as the slant-shear test (ASTM C 882 2013). ASTM C882 / C882M specifies that a cylindrical concrete specimen be used. In contrast, BS EN 12615 states that a cubical concrete specimen should be used. Unfortunately, these slant-shear methods were not developed to control bond line thickness; thus, in a cylindrical concrete specimen it is difficult to pin down the controlled slant gaps until the glue is completely cured because the cylindrical specimen has a tendency to roll. Thus, a cubical concrete specimen was selected, BS EN 12615. The shape and size of the specimen are shown in Table 7 and Figure 34.

Table 7 Size the Specimen

Cross section (a by a)	Total height (h)	Angle (α)	Bond line thickness (t)
$100 \times 100\ mm^2$	400 mm	30°	1mm ~ 7mm

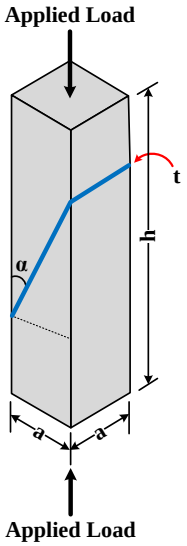

Figure 34 Conceptual Drawing of the Slant-Shear Test

5.2.2 Shear Stress Mechanism

To conduct the slant-shear test, a load had to be applied in the longitudinal direction of the specimen, rather than a force exerted in the slant direction at 30^{o} from the longitudinal direction of the specimen; the load had to be applied until the moment the layer began to slide. The following equation was used to convert the compressive stress into shear stress, and thus obtain the shear strength (Harris et al. 2015).

$$\tau_n = \frac{F}{A} \times \sin(\alpha) \times \cos(\alpha)$$

where τ_n is the shear stress, F is the load, A is the area, and α is the slant degree from the longitudinal direction of the specimen.

5.2.3 Specimen Material

Ultra-rapid hardening cement was used to conduct the test. Table 8 illustrates the material properties of the concrete specimen.

Table 8 Mechanical Properties of the Concrete Specimen (KQICI 2016)

Item	Age	Strength
Compressive Strength	2 Hours	26.1 MPa
	3 Hours	33.9 MPa
	1 Day	40.6 MPa
	3 Days	45.1 MPa
	7 Days	49.6 MPa
	28 Days	56.2 MPa
Flexural Strength	3 Hours	5.1 MPa
	1 Day	5.9 MPa

5.2.4 Bonding Agent Material

Three epoxy resin bonding agents were used in this study. Bisphenol A (YD 128) was used as an epoxy because it is highly adaptable and resistant to chemical substances and temperature changes (YD 128 2004). A modified aliphatic amine (KH 500) was applied as a hardener to make the first epoxy resin adhesive, because it quickly hardens at room temperature and has excellent chemical resistance (KH-500 2004). A modified cycloaliphatic amine (KH 816) was used to make another epoxy resin adhesive. This high gloss hardener is chemically resistant, and therefore proper to use in the tank lining (KH-816 2004). The final hardener was a modified aromatic amine (TH 451), which is frequently used as a bonding agent in civil structures because of its high

level of strength (TH-451 2004). The physical properties of the three types of epoxy resin adhesives are shown in Table 9.

Table 9 Physical Properties of Epoxy Resin Adhesives

	Epoxy	Hardener (Modified Type Amine)	Gel Time at 20°C (mins)	Peel Strength (MPa)	Tensile Strength (MPa)
1	Bisphenol A	Aliphatic	12	5.79	11.57
2		Cycloaliphatic	50	5.88	36.28
3		Aromatic	20	5.88	19.61

5.2.5 Joint Geometry and Surface Preparation for Slant-Shear Test

The area of the adherend was 200mm in width and 100mm in height; all joint geometry overlapped, as shown in Figure 36. The material of the adherend was concrete. The surface was cut with a grinder, and a brush was used to clean away foreign matter. To consider the worst-case scenario and determine the pure shear strength of the adhesive, all foreign matter was removed from the adherend.

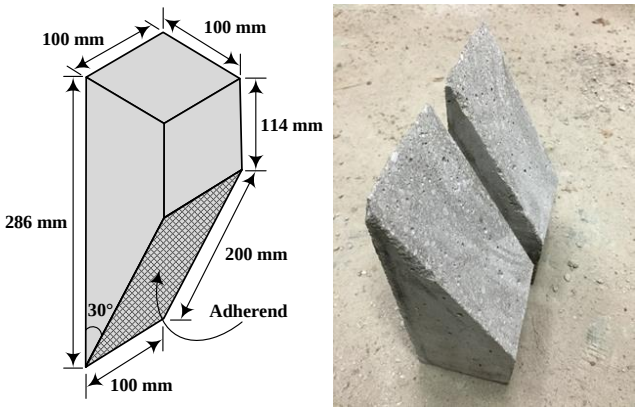

Figure 35 Joint Geometry and Surface Preparation

5.2.6 Assembly of Adhesive Joints

To remove eccentricity, it was essential that the specimen be attached in the same way as the original once the adhesive was applied. When an eccentric specimen is formed, the shear strength of the adhesive cannot be measured because the concrete breaks before the bond layer begins to slide. Therefore, cut concrete specimens were inserted into the mold to make it eccentricity-free. Then, a steel plate was added to remove the gap between the concrete adherends, in order to maintain the thickness of the bond. The glue was injected into the controlled gap to create a regulated bond line thickness, as shown in Figure 36.

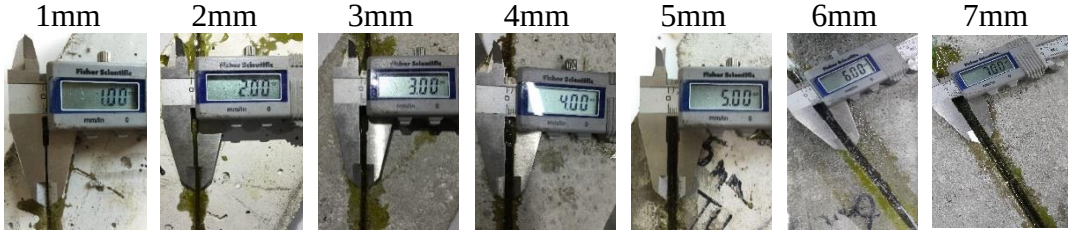

Figure 36 Controlled Bond Line Thickness

At this point, vinyl was wrapped around the specimens and both pieces were put in the mold to prevent the adhesive from flowing out of the regulated gap before the adhesive layer was set. If the vinyl did not tightly adhere to the specimens, the adhesive would leak out. C-clamps were used to tightly hold the vinyl between the mold and the concrete specimen to prevent leakage. Glue was filled in the controlled gaps and cured for three days at room temperature (20°C). When the adhesive was cured, a reference

bar was attached perpendicular to the bond line slant, as shown in Figure 37. The displacement was measured with an LVDT when the slant-shear test was executed.

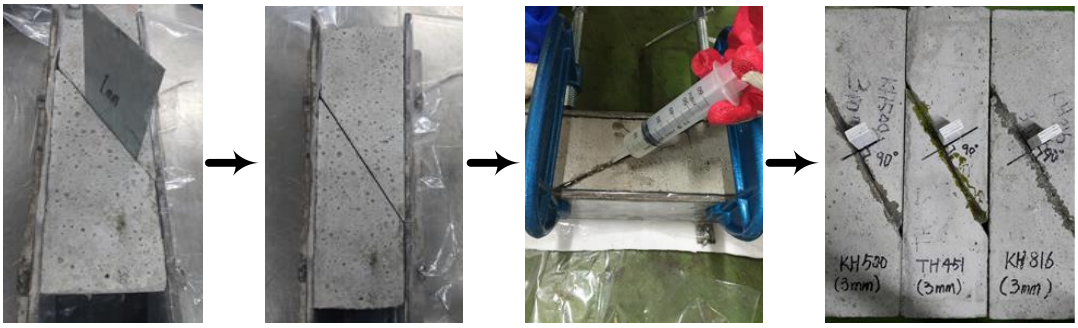

Figure 37 Assembly Sequence of the Slant-Shear Specimen

5.2.7 Number of Specimens

Three types of epoxy resin glue were used in this study. The layer thicknesses of the bonds were controlled to be between 1mm and 7mm, and there were five samples of each thickness. There were total of 35 specimens for each bond type, as shown in Table 10.

Table 10 Number of Specimens for the Slant-Shear Test

	Epoxy	Hardener (Modified Type Amine)	Number of Bond Line Thicknesses	Specimen Number for Each Thickness	Total Specimens
1	Bisphenol A	Aliphatic	7	5	35
2		Cycloaliphatic	7	5	35
3		Aromatic	7	5	35

5.2.8 Strain Measurements

Since epoxy resin is in liquid form, it is impossible to directly measure the strain. Instead, the displacement was measured through the mechanical definition of the shearing deformation rate, as shown in Figure 38 and the equation below. The spacing between the adherends of the upper and lower specimens was equal to the thickness of the bond layer. Since the height of the bond layer was fixed, the shear strain could be obtained by measuring the transverse displacement. The strain calculated in this study was the plastic deformation, because the displacement began in the plastic region when passing over the yield stress.

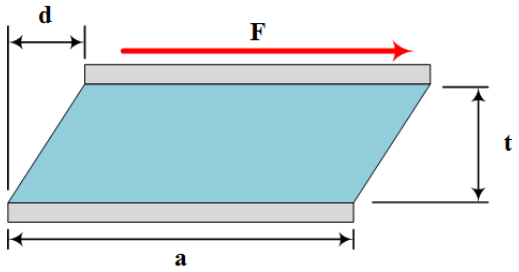

Figure 38 Shear Strain Mechanism (Gere 2004)

$$\text{Shear Strain} = \frac{\text{Shear Displacement (d)}}{\text{Bondline Thickness (t)}}$$

The perpendicular reference bar attached to the longitudinal direction of the bond line used LVDT to measure the transverse displacement, as shown in Figure 39. The shear strain was determined through the displacement measurements, according to each

bond line thickness. Once the shear strain was identified, the shear stress/shear strain could be calculated.

Figure 39 Reference Bar for Measuring the Transverse Displacement

5.2.9 Mechanical Testing of the Adhesive Joints

After the glue was completely cured, the concrete specimen was placed in the UTM (Model: HD-201) and the slant-shear test was carried out. The load was 2.3 ton/min; it was applied until the moment the layer began to slide. The failure mode of the slant-shear test with the LVDT setup is shown in Figure 40.

Figure 40 Slant-Shear Test with LVDT Setup

5.3 Results of the Stress-Strain Relationship Analysis

5.3.1 Epoxy Resin Glue 1: Bisphenol A with Modified Aliphatic Amine

The first epoxy resin adhesive used bisphenol A and a modified aliphatic amine. When the bond line thickness increased from 1mm to 7mm, the relationship between the shear stress and shear strain appeared, as shown in Figure 41. As a result, the shear stress came to a maximum at 4mm, but the shear strength fell sharply at a bond thickness of 6mm, and was minimal at 7mm. It also appeared that the transverse displacement was less when the shear strength was high. This means that when the strength of the epoxy resin adhesive was strong, there was little displacement. Also, a brittle fracture appeared without any signs of destruction.

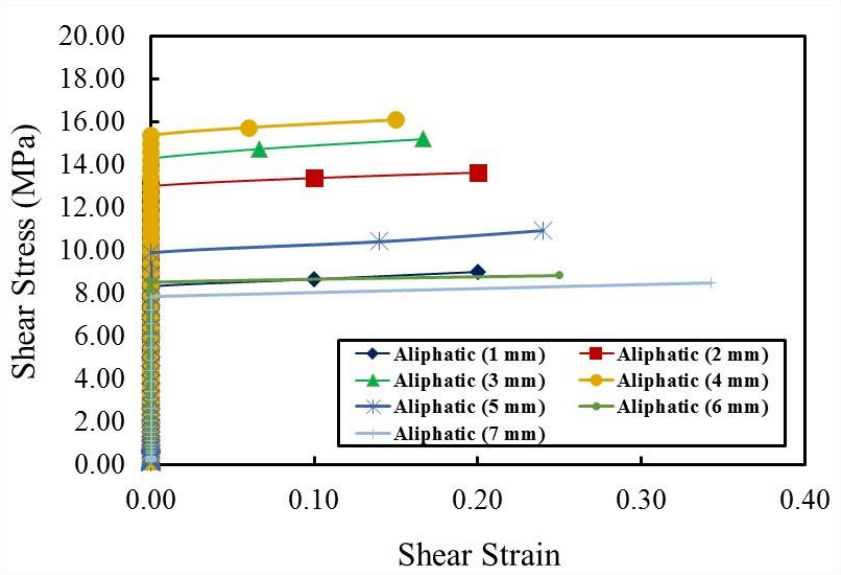

Figure 41 Relationship of Shear Stress to Shear Strain in Adhesive 1

5.3.2 Epoxy Resin Glue 2: Bisphenol A with Modified Cycloaliphatic Amine

The second epoxy resin adhesive used bisphenol A and a modified cycloaliphatic amine. Also, as with the first glue, the thickness was a variable. The result of the experiment was that maximum shear stress developed when the thickness of the bond line was 4mm, as shown in Figure 42. The shear stress was reduced dramatically when the bond line thickness was 6mm. The minimum shear stress developed when the height of the bond layer was 7mm. As with the first glue, the shear strain was not particularly large when the strength of the glue was high. It was also evident that the shearing failure occurred immediately after the displacement.

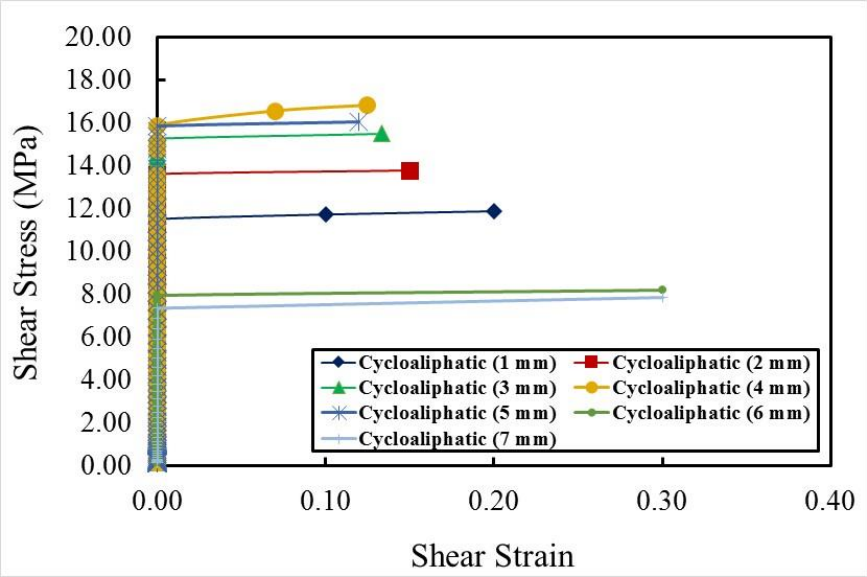

Figure 42 Relationship of Shear Stress and Shear Strain in Adhesive 2

5.3.3 Epoxy Resin Glue 3: Bisphenol A with Modified Aromatic Amine

The third epoxy resin adhesive used bisphenol A and a modified aromatic amine. The results of this experiment were the same as those for glues 1 and 2, in that the maximum shear stress developed when the thickness of the bond line was 4mm (see Figure 43). The reason why the shear strain of glue 3 was less than that of glues 1 and 2 is that the shear strength of glue 3 was higher than that of the other two adhesives.

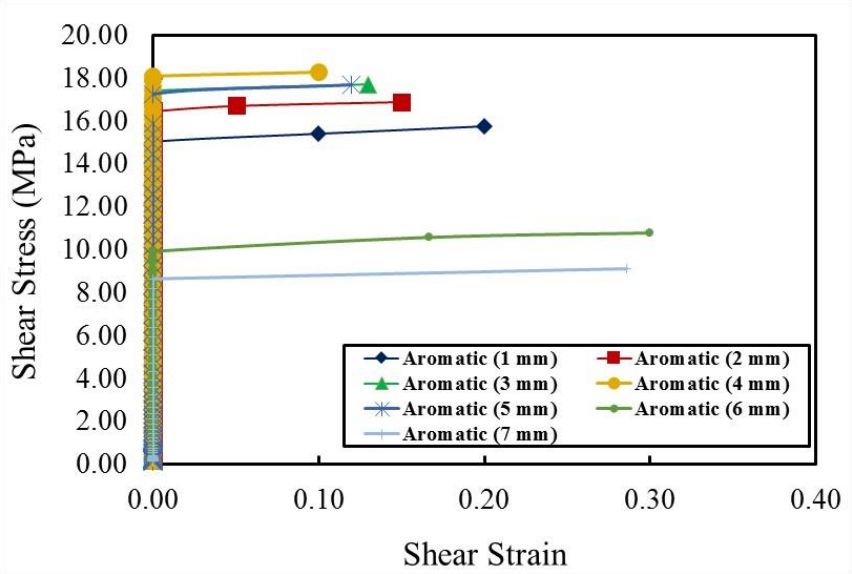

Figure 43 Relationship of Shear Stress and Shear Strain in Adhesive 3

5.3.4 Comparison of the Three Epoxy Resin Adhesive Shear Strengths

The three adhesives were compared to determine the relationships among the three bond thicknesses and three glue shear strengths, as shown in Figure 44. The results

indicate that all three bonds had similar tendencies. The maximum shear strength was when the thickness of the bond was 4mm; it rapidly diminished at 5mm and beyond. In general, the overall shear strength was higher when bisphenol A was used as the epoxy and the modified aromatic amine was used as the hardener. Table 11 shows the values of average shear strength regarding bond line thickness.

Table 11 Average Ultimate Shear Strength Regarding Bond Line Thickness (Unit: MPa)

Thickness	1 mm	2 mm	3 mm	4 mm	5 mm	6 mm	7mm
Adhesive 1	9.90	13.84	15.27	15.93	11.04	9.61	8.55
Adhesive 2	11.66	15.07	17.20	17.51	17.29	8.42	7.98
Adhesive 3	15.30	16.55	17.96	18.94	18.20	10.67	9.39

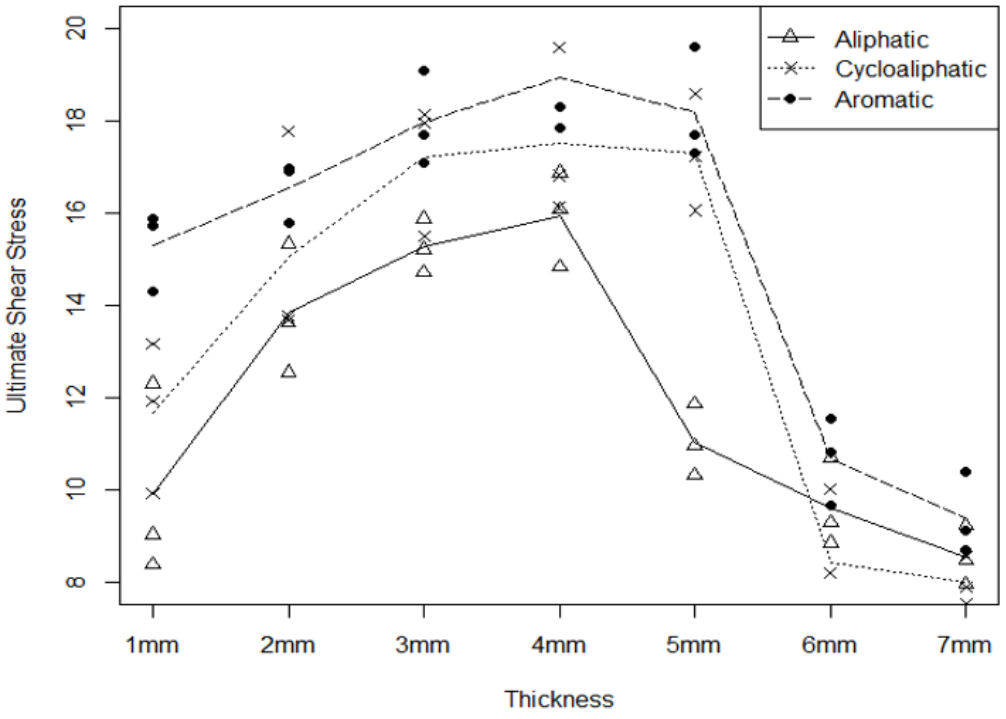

Figure 44 Comparison of the Three Epoxy Resin Adhesive Shear Strengths

5.3.5 Mechanism of the Epoxy Resin Adhesive with the Concrete Structure

All materials have a plastic deformation that does not allow the material to return to its original condition when the load exceeds a certain amount of resistance force. When force is applied to the epoxy resin bonding agent, it cannot move beyond the yield stress. The deformation occurs when the forces pass beyond the yield stress limit of the bonding agent. The shear strain is zero until it reaches the yield stress of the epoxy resin glue. A shear strain occurs at the moment the loading passes beyond the yield stress that does not allow the glue to return to its initial condition. In other words, there is a slight resistance at the beginning, and ultimate shear failure occurs immediately after loading beyond the yield stress as shown in Figure 45.

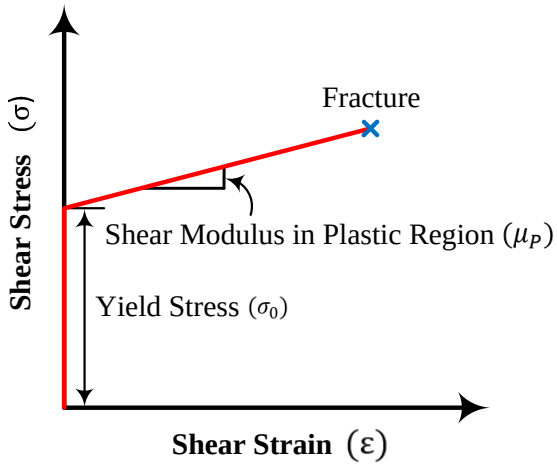

Figure 45 Mechanism of the Epoxy Resin Adhesive with the Concrete Structure

The mechanical behavior of the epoxy resin adhesive (Type IV) is illustrated in Figure 45. Since the strain did not occur until the load reached the yield stress, the yield

stress was presented on the y-axis, as the intercept. The ultimate shear stress increased as much as the amount of the shear modulus in the plastic region, after the loading reached the yield stress. This tendency was linear, as shown below:

$$\sigma = \sigma_0 + \mu_P \times \varepsilon$$

where the ultimate shear stress is σ, the yield stress is σ_0, the shear modulus in the plastic region is μ_P, and the shear strain is ε.

5.3.6 Mathematical Relationship Between the Bond Line Thickness and Ultimate Shear Stress of the Epoxy Resin Adhesive

The relationship between the bond line thickness and the ultimate shear stress was established by the following mathematical relationship. Here, the shear strain of the bond line refers to the distance at which the shear failure occurred at the thickness of the bond layer and slid transversally. Therefore, the mechanical relationship can be expressed as follows:

$$\sigma = \sigma_0 + \mu_P \times \frac{d}{h}$$

where the ultimate shear stress is σ, the yield stress is σ_0, the shear modulus in the plastic region is μ_P, the displacement is d, and the bond line thickness is h.

The mean values obtained through the experiment are shown in Table 12. If the average value obtained is substituted into each corresponding variable, the mutual relationship between the bond line thickness and ultimate shear stress for each adhesive can be mathematically explained. The ultimate shear stresses of the corresponding bonds can be determined by substituting the bond line thickness through the determined mathematical relationships.

Table 12 Average Values of Each Variable

Epoxy Resin Adhesive	Average Yield Stress (MPa)	Average Modulus of Plastic	Average Displacement (mm)
Adhesive 1	11.09	4.54	0.10
Adhesive 2	12.38	7.19	0.09
Adhesive 3	14.76	3.41	0.08

The mathematical relationship between the bond line thickness and ultimate shear stress for each adhesive, when substituting data values for each variable, is as follows:

- Adhesive 1: Bisphenol A – Modified Aliphatic Amine

$$\sigma = 11.09 + 4.54 \times \frac{0.10}{h}$$

- Adhesive 2: Bisphenol A – Modified Cycloaliphatic Amine

$$\sigma = 12.38 + 7.19 \times \frac{0.09}{h}$$

- Adhesive 3: Bisphenol A – Modified Aromatic

$$\sigma = 14.76 + 3.41 \times \frac{0.08}{h}$$

Three adhesives were used in this study. Each bond line thickness was controlled from 1mm to 7mm. Five concrete specimens were prepared for each bond line thickness. If the number of concrete specimens was at least 30 for each bond line thickness (satisfying the central limit theorem), the data distribution would be normal and the proposed mathematical relationships between the bond line thicknesses and the ultimate shear strengths could be expressed with confidence (Penn State 2017). However, in order to meet the central limit theorem, total 630 concrete specimens had to be made, which was not realistic or practical. For this study three epoxy-resin adhesives are used, the bond line thickness is controlled from 1 mm to 7 mm, and thirty concrete specimens are required for each bond line thickness.

Total number of concrete specimens are as follows:

= Number of Adhesives that used for this study × Number of Bond Line Thickness × Number of Specimen for Each Bond Line Thickness = 3 × 7 × 30 = 630 Specimens

Yet the proposed mathematical relationship was sufficient to show the tendency of the mechanical association between the ultimate shear strength and the bond line thickness.

5.3.7 Stress Increment Analysis of the Plastic Region

Deformation of the bond line occurs only once the yield stress is reached. This means that abnormalities in the attached concrete patch cannot be identified with the naked eye. Anomalies can be recognized with the naked eye only once the resistance force is reached in the plastic region. However, it is possible to lose the structural stability of the glue, because at this point the resistance force has already exceeded the elastic region. Accordingly, when abnormalities can be clearly seen, the adhesive should be reapplied or the area should be re-repaired via another method. If sufficient resistance strength appears in the plastic region, a time can be scheduled to fix the damage again.

Since the plastic region's bond strength is unknown, this section discusses the resistance strengths of the applied glues in this space. To determine the shear strengths

of the three epoxy resin adhesives employed in this research, this study analyzed how much the glue's strength increased from the average yield shear stress to the average ultimate shear stress. The values of the yield shear stress were removed from those of the ultimate shear stress to determine the increased amount of resistance force in the plastic region. In order to determine whether the resistance force occupied an important part of the overall shear stress, the proportion of shear stress in the plastic region was examined via the following expression.

$$\text{Stress in Plastic Region} = \text{Ultimate Shear Stress} - \text{Yield Stress}$$

$$\text{Percentage of Plastic Region} = (\text{Stress in Plastic Region} \div \text{Ultimate Shear Stress}) \times 100\%$$

First, the average strength of the first epoxy resin adhesive increased as much as 1.12 MPa in the plastic region. This accounts for 8.89% of the ultimate shear stress; its unique values are shown in Table 13.

Table 13 Values of Stress Increments in the Plastic Region (Adhesive 1)

Epoxy Resin Adhesive (Bisphenol A – Modified Aliphatic Amine)								
Bond Line Thickness (mm)	1	2	3	4	5	6	7	Average
Stress in Plastic Region (MPa)	0.73	1.30	1.61	1.96	1.00	0.77	0.49	1.12
Percentage of Plastic Region (%)	7.34	9.37	10.52	12.32	9.06	7.88	5.73	8.89

Stress in the plastic region increased when as the maximum shear strength increased. Conversely, a reduction in the ultimate shear strength was also shown to reduce shear stress in the plastic region, as shown in Figure 46.

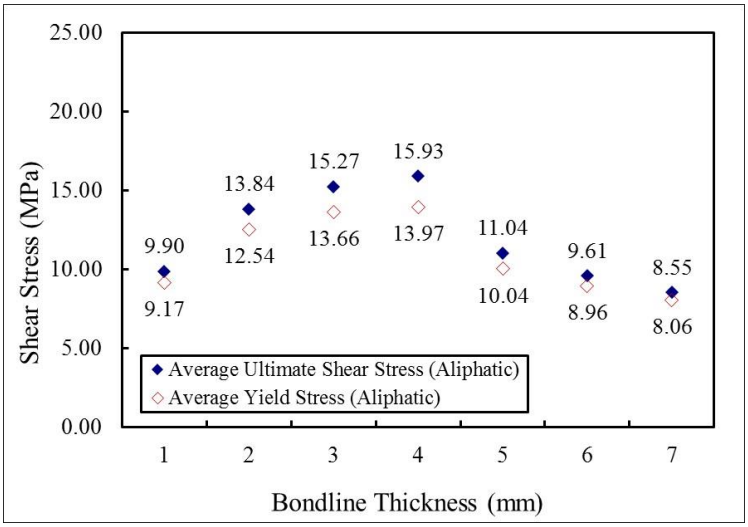

Figure 46 Trend of Stress Increments in the Plastic Region of Adhesive 1

The average increased shear stress in the plastic region of the second epoxy resin adhesive was 1.01 MPa. This accounted for 7.58% of the ultimate shear stress; the corresponding values for each bond line thickness are shown in Table 14.

Table 14 Values of Stress Increments in the Plastic Region (Adhesive 2)

Epoxy Resin Adhesive (Bisphenol A – Modified Cycloaliphatic Amine)								
Bond Line Thickness (mm)	1	2	3	4	5	6	7	Average
Stress in Plastic Region (MPa)	0.60	1.13	1.26	1.59	1.24	0.76	0.52	1.01
Percentage of Plastic Region (%)	5.12	7.52	7.35	9.10	7.15	10.03	6.5	7.58

The results of the second epoxy resin adhesive are similar to those of the first glue, as shown in Figure 47. However, there was no greater stress on the plastic region than what was seen with the first bonding agent. This means that once the load entered the plastic region, a brittle fracture immediately occurred.

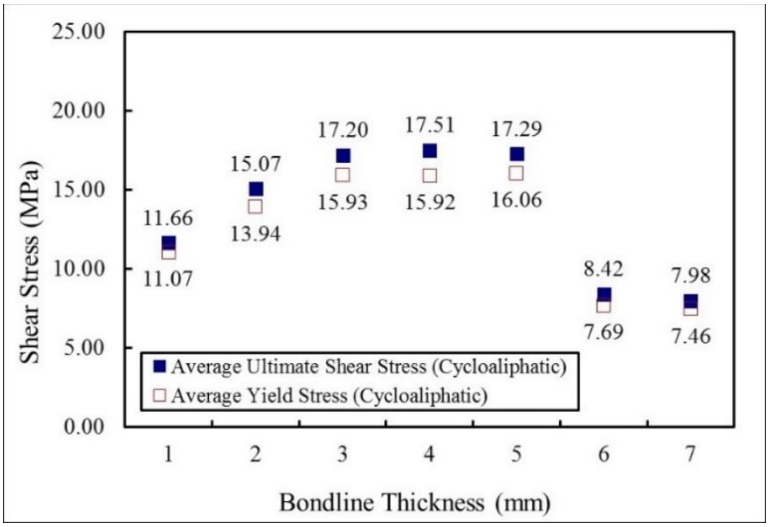

Figure 47 Trend of Stress Increments in the Plastic Region of Adhesive 2

The average value of the increased shear stress in the plastic region of the third epoxy resin adhesive was 0.81 MPa. This represented 5.42% of the ultimate shear stress; the corresponding values of the bond line thicknesses are shown in Table 15.

Table 15 Values of Stress Increments in the Plastic Region (Adhesive 3)

Epoxy Resin Adhesive (Bisphenol A – Modified Aromatic Amine)								
Bond Line Thickness (mm)	1	2	3	4	5	6	7	Average
Stress in Plastic Region (MPa)	0.44	0.73	0.89	1.23	1.11	0.86	0.44	0.81
Percentage of Plastic Region (%)	2.85	4.41	4.95	6.49	6.12	8.45	4.7	5.42

The third epoxy resin adhesive was similar to the first and second adhesives, as shown in Figure 48. However, considering that the stress increase in the plastic region of the third adhesive was smaller than that of the first and second adhesives, the majority of the loads were dealt with in the yield stress; a brittle fracture occurred in the plastic region once the applied load was over the yield stress.

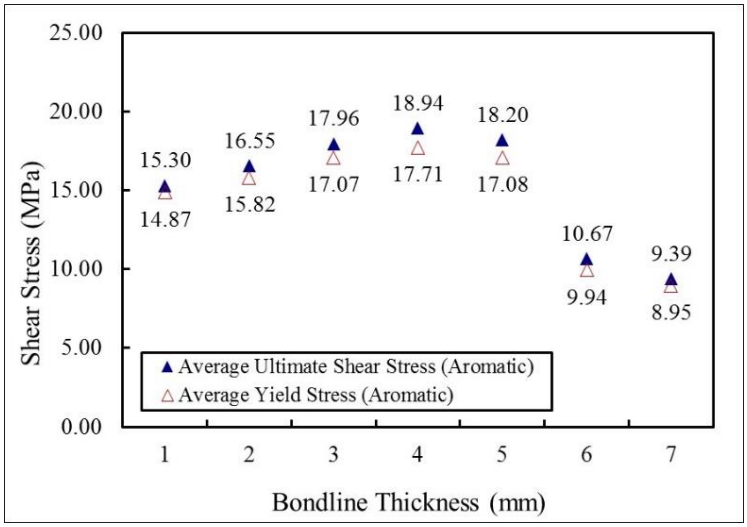

Figure 48 Trend of Stress Increments in the Plastic Region of Adhesive 3

For all three adhesives, the increased amount of stress in the plastic region was not particularly substantial. Consequently, when the epoxy resin adhesive was applied to the concrete structure, the yield stress tended to be resistant to any applied force. It was also found that the stress in the plastic region was small compared to the ultimate shear stress, though some stress did occur in the plastic region. This indicates that abnormal symptoms tended not to be visible to the naked eye, and thus would not allow enough time to make a decision to re-repair. Brittle fractures occurred immediately after

the yield stress was exceeded, and it is expected that such fractures would result in the patch coming off. In addition, it was found that the yield stress and stress in the plastic region improved when there was a gap between the concrete segments. For example, when attaching a hardened concrete patch, it was more advantageous to repair the spall than carry out a precise machining operation to fit it.

5.3.8 Ultimate Shear Displacement by Bond Line Thickness

Three epoxy resin bonding agents were used to analyze how the thickness of the bond layer affects the displacement. It was found that as the bond line thickness increased, the shear displacement showed a nonlinear relationship, as shown in Figure 49; however, the trend was increased. The shear displacement of the specimen increased as the epoxy resin bond line thickness applied to the concrete increased.

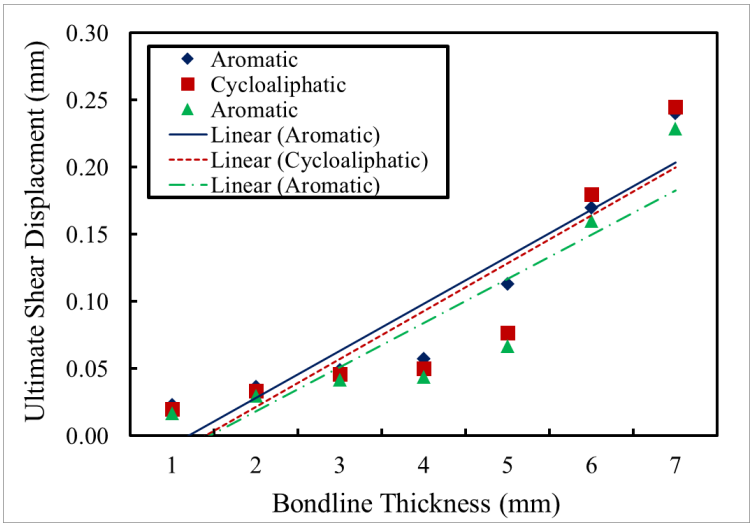

Figure 49 Relationship between Bond Line Thickness and Ultimate Shear Displacement

The overall trend of the above three epoxy resin (Type 4) adhesives was largely divided into two sections, as shown in Figure 50 and Figure 51, with linear relationships between 1mm ~ 4mm and 5mm ~ 7mm, respectively. The increase in the displacement was small when the bond line thickness increased from 1mm to 4mm, but the increase in the displacement was large when the thickness of the bond layer increased from 5mm to 7mm. This meant that the strength increased from 1mm to 4mm when compared with the shear strength analysis. However, the strength of the bond decreased and the displacement increased sharply when the thickness of the bond line exceeded 5mm. As a result of the analysis, it could be seen that the performance of the bond was generally unstable when the thickness of the bond layer exceeded 5mm.

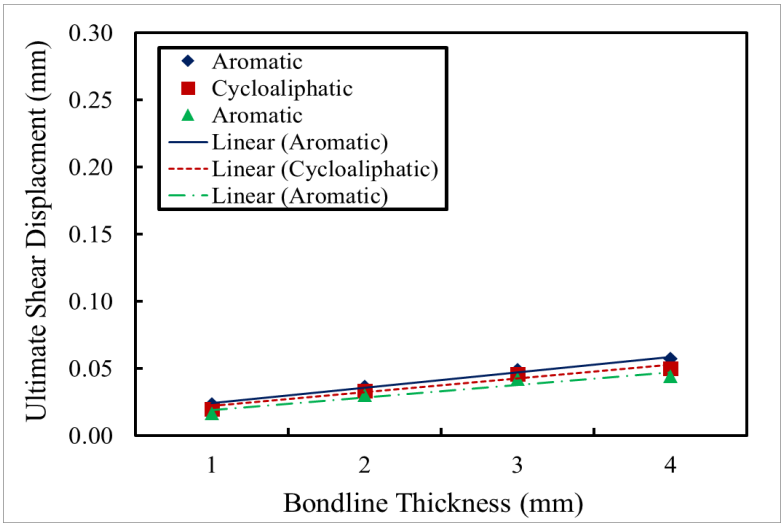

Figure 50 Relationship between Bond Line Thickness and Ultimate Shear Displacement (1mm ~ 4mm)

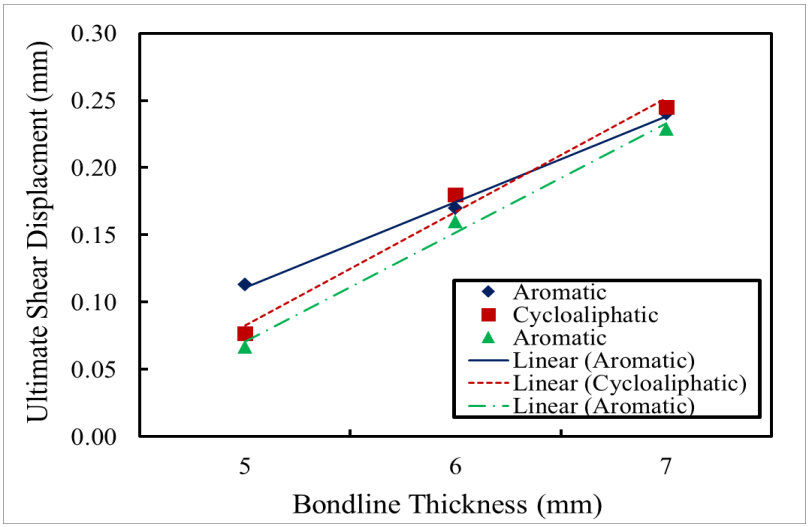

Figure 51 Relationship between Bond Line Thickness and Ultimate Shear Displacement (5mm ~ 7mm)

5.3.9 Failed Bonding Interface Analysis

The adhesive's failure state was analyzed after the slant-shear test was executed, in order to determine whether a shear failure occurred. Figure 52 shows the state of the adhesive surface after the shear failure of the first adhesive, which in this experiment used a modified aliphatic amine as a hardener. Figure 53 shows the state of the adhesive surface when a modified cycloaliphatic amine was used as a hardener. Figure 54 shows the state of the adhesive surface after shear failure when a modified aromatic amine was used as a hardener.

Figure 52 Crumpling Epoxy Resin Adhesive 1

Figure 53 Crumpling Epoxy Resin Adhesive 2

Figure 54 Crumpling Epoxy Resin Adhesive 3

The mechanism for when shear failure occurs in the bond layer is shown in Figure 55. Until the shearing force (F) reaches the yield stress, the displacement (d) does not occur without changing the bond layer, but instead exceeds the yield stress and reaches the plastic region. At this time, the bond layer is stretched in a transverse direction and the bond line is crumpled.

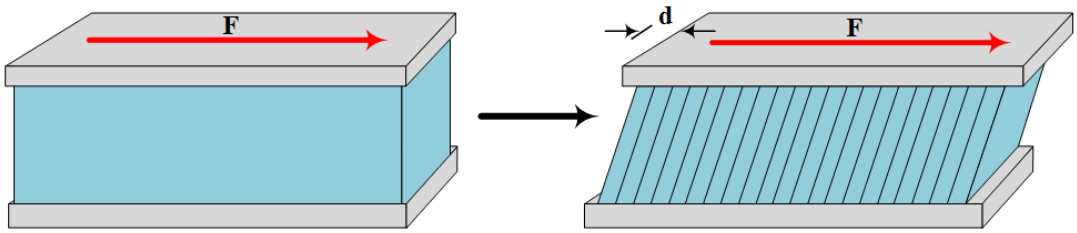

Figure 55 Crumpling of the Bond Line by Transverse Displacement

Traces of the remaining bond visibly crumpling serves as evidence that shear failure has occurred. However, if there are no stripe marks, it is difficult to determine if shear failure has occurred.

6. DISCUSSION

6.1. Discussion of Results of Slant Shear Test

This is because when the epoxy resin was applied to the concrete, the yield stress dealt with most of the applied load. When the yield stress was applied to the concrete specimen, no strain was found. The shear deformation began to occur at the moment the stress exceeded the yield stress. Then, the load entered the plastic region and the structure did not return to its original state. In the plastic region, the resistive force was a minor stress compared to the yield stress, so that the resistance stress in the plastic region did not handle the applied stress. This phenomenon was clearly different from previous studies of shear stress measurement when an epoxy resin bond was applied to a steel plate, as in the Arcan test. The shear resistance tended to increase when the thickness of the bond line increased from 1mm to 4mm, and the shear resistance decreased when the bond line thickness exceeded 4mm. This proved that the results were different from the shear stress tendencies shown in existing epoxy resin adhesives studies.

6.2. Discussion of Structural Sustainability of the Glued Concrete Segment

In general, the overall shear strength is higher when bisphenol A is used as an epoxy and aromatic amine modified type is used as a hardener. The minimum shear

strength of this adhesive is about 1 MPa smaller than the maximum shear stress by a container truck shown as follow:

Maximum applied shear stress along the bond layer by a container truck

– Ultimate shear strength of adhesive 3 (Bisphenol A - Aromatic amine modified type)

= 16.40 MPa - 15.30 MPa = 1.10 MPa

The standard load used in the road design is the single axis of the container truck. This is about 9,000 kg. With the vertical load of this single axis of the container, we need to think about something. According to the result of comparison between the applied stress and bond strength, concrete patches will fall off from the spall if there is a very unusual situation in which the container truck continues to accelerate rapidly on the concrete segment or stops suddenly on top of the concrete segment. However, this assumption is rare in real situations. Also, the epoxy-resin glue that has a higher strength can be applied than the adhesive of examined shear strength in order to handle every spall. Therefore, the spall repair method using 3D printer is sufficiently realistic from a structural point of view.

7. CONCLUSION

Although epoxy resin adhesives are widely used in concrete structures, the amount of adhesive applied to a concrete surface is not commonly considered. Also, currently there is no study on how shear strength varies when the thickness of the bond line applied to a concrete structure is changed. Hence, this research is unique.

The epoxy-resin glue that has a higher strength can be applied rather than the adhesive used in the examination of shear strength in order to handle every spall. Also, the selection of high-strength adhesives is essential because epoxy resin adhesives break down immediately (brittle fraction) without a sign of structural instability.

Moreover, it was found that the concrete patches had better adhesion strength than the ones that completely fit the damage. Cumulative errors by 3D scanning and 3D printing technologies are better than when there is no error in generating a concrete segment that fits into the spall perfectly.

Also, it is expected that the spall repair method using 3D printing that is suggested in this study can reduce the amount of time of road blockage because the gel set time is less than an hour.

In addition, the spall repair method using a 3D printer is sufficiently realistic from a structural point of view, except in unusual situations.

Finally, the tendency of the ultimate shear strength of three epoxy-resin adhesives that were used in this study can be forecast when the measured bond line thickness is applied to the variable of the determined mathematical relationships of each

adhesive. These mathematical relationships can be utilized if users care to identify the ultimate shear strengths of epoxy resin adhesives without engaging in complicated numerical analyses or costly experiments when they plan to use the three epoxy-resin adhesives (1. Bisphenol A - Aliphatic Amine Modified Type, 2. Bisphenol A - Cycloaliphatic Amine Modified Type, 3. Bisphenol A - Aromatic Amine Modified Type) that were examined in this study.

8. FUTURE WORK

The tolerances of 3D scanning and printing technologies can be compensated for with bond line thickness when the glued surface of a concrete segment is put upside-down on a spall, as shown in Figure 56. The bounds of bond line thickness should be defined based on the sum of the tolerance of the 3D scanning technology and tolerance of the 3D printing technology, as shown below. Future research should endeavor to determine the bond line thickness created by the tolerances of the 3D scanner and printer. Moreover, this study illustrates a method of determining the corresponding ultimate shear strength among the determined ultimate shear strengths of epoxy resin adhesives.

Bounds of Bond Line Thickness = Tolerance of 3D scanner + Tolerance of 3D Printer

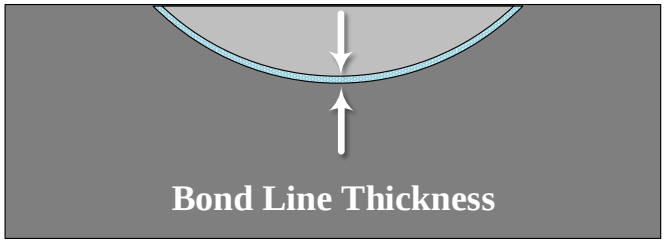

Figure 56 Bounds of Bond Line Thickness

REFERENCES

Afendi, M. (2011). *Study on effect of bond thickness upon adhesive strength and fracture characteristics of brittle epoxy adhesively bonded dissimilar joint*, University of Tsukuba, Tsukuba.

Arenas, J. M., Narbon, J. J., Alia, C. (2010). "Optimum adhesive thickness in structural adhesives joints using statistical techniques based on Weibull distribution." *Int. J. of Adh. and Adh.*, 30, 160-165.

ASTM C881. (2015). *Standard specification for epoxy-resin base bonding systems for concrete*, American Society Testing and Materials International, West Conshohocken.

ASTM C 882. (2013). *Standard test method for bond strength of epoxy-resin systems used with concrete by slant shear*, American Society Testing and Materials International, West Conshohocken.

Aydin, S., Solmaz, M., Turgut, A. (2012). "The effects of adhesive thickness, surface roughness and overlap distance on joint strength in prismatic plug-in joints attached with adhesive." *Int. J. of the Phy. Sci.*, 7(17), 2580-2586.

Banea, M. D., Silva, L. F., Campilho, R. D. (2015). "The effect of adhesive thickness on the mechanical behavior of a structural polyurethane adhesive." *J. of Adh.*, 91, 331-346.

Basham, D., Wright, J., Ferguson, K., Moy, G. (2001). *Concrete crack and partial-depth spall repair*, US Department of Defence, Virginia.

Bobo, J. (2003). *Crash reconstruction basic for prosecutors*, American Prosecutors Research Institute, Alexandria.

Broughton, B., and Gower, M. (2001). *Preparation and testing of adhesive joints*, National Physical Laboratory Materials Centre, Teddington.

Bryant, R. W., and Dukes, W. A. (1967). "The effect of joint design and dimensions on adhesive strength." *Soc. of Auto. Eng.*, 10, 1-9.

BS EN 12615. (1999). *Products and systems for the protection and repair of concrete structures: test methods - determination of slant shear strength*, British Standards Institution., London.

Carr, K. (2009). "7 key features of the 3 shape dental system." *LMT*, <http://lmtmag.com> (Sep. 1, 2016).

Chai, H. (1993). "Deformation and failure of adhesive bonds under shear loading." *J. of Mat. Sci.*, 28, 4944-4956.

Chai, H. (2004). "The effects of bond thickness, rate and temperature on the deformation and fracture of structural adhesives under shear loading." *Int. J. of Frac*., 130, 497-515.

Ciobanu, O., Xu, W., Ciobanu, G. (2013). "The use of 3D scanning and rapid prototyping in engineering." *J. of. Fiab. & Dura*., 1, 241-247.

Ciocca, L., and Scotti, R. (2004). “CAD-CAM generated an ear cast by means of a laser scanner and rapid prototyping machine.” *J. of Pro. Den*., 92, 591-595.

Ciocca, L., Mingucci, R., Gassino, G., Scotti, R. (2006). “CAD/CAM ear model and virtual construction of the mold.” *J. of Pro. Den*., 98, 339-343.

Dai, F., and Lu, M. (2008). “Photo-based 3D modeling of construction resources for visualization of operations simulation: case of modeling a precast facade.” *Proc., the 2008 Winter Simulation Conference*, IEEE, Miami, FL, 2439-2446.

Davies, P., Sohier, L., Cognard, J.-Y., Bourmaud, A., Choqueuse, D., Rinnert, E., Creachcadec, R. (2009). “Influence of adhesive bond line thickness on joint strength.” *Int. J. of Adh. and Adh*., 29(7), 724-736.

Ellysa, C. (2015). “Research in education and the behavioral / social science.” *Penn State University*, <http://psu.libguides.com> (Apr. 15, 2016).

FHA. (1994). “Partial-depth repair of concrete pavement.” *Federal Highway Administration*, <https://www.youtube.com/watch?v=b6xWvWCLC5E> (Jan. 21, 2015).

Fowler, D., Zollinger, D., Whitney, D. (2008). *Implementing best concrete pavement spall repairs*, Center of Transportation Research, Austin.

Fuster-Torres, A., Albalat-Estela, S., Alcaniz-Raya, M., Penarrocha-Diago, M. (2009). “CAD/CAM dental systems in implant dentistry: Update.” *J. of Ora. Surg*., 14(3), 141-145.

Gere, J. (2004). *Mechanics of materials*, 6th Ed., Thomson, Belmont.

Gleich, D. (2002). *Stress analysis of structural bonded joints*, Imperial College, Guildford.

Gonzalez-Jorge, H. (2012). "Photogrammetry and laser scanner technology applied to length measurements in car testing laboratories." *J. of Meas*., 45, 354-363.

Harris, D. K., Munoz, M. A., Gheitasi, A., Ahlborn, T. M., Rush, S. V. (2015). "The challenges related to interface bond characterization of ultra-high-performance concrete with implications for bridge rehabilitation practices." *J. of Adv. in C. Eng. Mat.*, 75-101.

He, Y., Xue, G.-h., Fu, J.-z. (2014). "Fabrication of low cost soft tissue prostheses with the desktop 3D printer." *Sci. Rep*., 4(6973), 1-7.

Hernanadez, D. (2015). "Factors affecting dimensional precision of consumer 3D printing." *Int. J. of Avi., Aero., and Aero*., 2(4), 1-43.

Houben, I. (2009). *Structural design of pavements*, Delft University of Technology, Delft.

Jarry, E., and Shenoi, R. A. (2006). "Performance of butt strap joints for marine applications." *Int. J. of Adh. and Adh*., 26, 162-176.

Jin, Y.-a., He, Y., Xue, G.-h., Fu, J.-z. (2015). "A parallel-based path generation method for fused deposition modeling." *Int. J. of Adv. Manu. Tech*., 927-937.

Kasparova, M., Grafova, L., Dvorak, P., Dostalova, T., Prochazka, A., Eliasova, H., Kakawand, S. (2013). “Possibility of reconstruction of dental plaster cast from 3D digital study models.” *J. of Biomed. Eng*., 12(49), 1-11.

KH-500. (2004). “Aliphatic amine modified type.” *Kukdo Chemical Co., Ltd*., <http://www.kukdo.com> (Aug. 2, 2016).

KH-816. (2004). “Cycloaliphatic amine modified type.” *Kukdo Chemical Co., Ltd*., <http://www.kukdo.com> (Aug. 2, 2016).

KQICI. (2016). *Test report of rapid hardening cement concrete*, Korea Quality Institute of Construction Industry, Yong-In.

Liacouras, P., Garnes, J., Roman, N., Petrich, A., Grant, G. (2010). “Designing and manufacturing an auricular prosthesis using computed tomography, 3-dimensional photographic imaging, and additive manufacturing: A clinical report.” *J. of Pro. Den*., 105(2), 78-82.

Liang, Y. M., and Liechti, K. M. (1996). “On the large deformation and localization behavior of an epoxy resin under multiaxial stress states.” *Int. J. of Sol. Strc*., 33(10), 1479-1500.

Lisa, G. (2008). *Qualitative research methods*, Sage Publication, Los Angeles.

Liu, P.-R. (2005). “Panorama of dental CAD/CAM restorative systems.” *Com. of Con. Edu. in Den.*, 26(7), 507-513.

Mailvaganam, N. (1997). “Effective use of bonding agents.” *Institute for Research in Construction*, <https://www.nrc-cnrc.gc.ca> (Jul. 4, 2016).

McVay, M. (1988). *Spall damage of concrete structures*, Department of the Army, Mississippi.

Miyazaki, T., Hotta, Y., Kunii, J., Kuriyama, S., Tamaki, Y. (2009). “A review of dental CAD/CAM: current status and future perspectives from 20 years of experience.” *J. of Den. Mat*., 28(1), 44-56.

Mormann, W. H., and Bindl, A. (1996). “The new creativity in ceramic restorations: dental CAD-CIM.” *J. of Quin. Int*., 27, 821-828.

Noort, R. (2012). “The future of dental devices is digital.” *J. of Den. Mat*., 28, 3-12.

Norman, D., and Yvonna, L. (2000). *Handbook of qualitative research*, Sage Publications, Los Angeles.

PCA. (2001). *Concrete slab surface defects: causes, prevention, repair*, Portland Cement Association, New York.

Penn State. (2017). “Confidence intervals and the central limit theorem.” *Penn State University*, <https://onlinecourses.science.psu.edu> (Feb. 3, 2017).

Scott, C. (2016). “A palace ceiling, a winged bull and a room full of history: 3D printed replicas of war-destroyed artifacts on display at roman colosseum.” *3D Print.com*, <https://3dprint.com> (Dec. 5, 2016).

Silva, L., Carbas, R., Critchlow, G. W., Figueiredo, M., Brown, K. (2009). “Effect of material, geometry, surface treatment and environment on the shear strength of single lap joints.” *Int. J. of Adh. & Adh*., 29 (6), 621-632.

TH-451. (2004). “Aromatic amine modified type.” *Kukdo Chemical. Co., Ltd*., <http://www.kukdo.com> (Aug. 2, 2016).

Tomblin, J. S., Yang, C., Harter, P. (2001). *Investigation of thick bondline adhesive joints*, US Department of Transportation, Washington DC.

US DoT. (2003). *Distress identification manual for the long-term pavement performance program*, US Department of Transportation, Washington DC.

US DoT. (2008). *Concrete pavement preservation workshop*, US Department of Transportation, Washington DC.

US DoT. (2013). “Commercial vehicle size and weight program.” *US Department of Transportation*, <http://ops.fhwa.dot.gov> (Apr. 7, 2016).

US DoT. (2014). “Concrete pavement design.” *US Department of Transportation*, <http://international.fhwa.dot.gov> (Apr. 9, 2016).

US DoT. (2015). “Work zone road user costs.” *US Department of Transportation*, <http://ops.fhwa.dot.gov> (Dec. 12, 2015).

Williams, R. J., Bibb, R., Eggbeer, D., Collis, J. (2006). “Use of CAD/CAM technology to fabricate a removable partial denture framework.” *J. of Pro. Den*., 96(2), 96-99.

YD 128. (2004). “Standard liquid epoxy resin.” *Kukdo Chemical. Co., Ltd*., <http://www.kukdo.com> (Aug. 2, 2016).